NAVY DEPARTMENT

THE DAVID W. TAYLOR MODEL BASIN

WASHINGTON 7, D.C.

HYDROSTATIC PRESSURE TESTS ON THIN RECTANGULAR DIAPHRAGMS 21 INCHES BY 13 1/2 INCHES

by

John W. Day

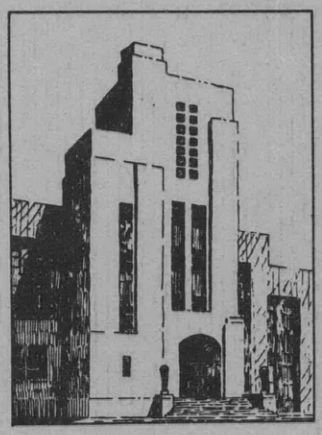

March 1951

Report 635

NS 724-008

INITIAL DISTRIBUTION

Copies

8 Chief, BuShips, Project Records (Code 362), for distribution:

- 5 Project Records
- 1 Technical Assistant (Code 106)
- 2 Underwater Explosion Research (Code 423)

2 Commander, Norfolk Naval Shipyard, Portsmouth, Virginia,

Attn: Underwater Explosions Research Unit, Code 205

TABLE OF CONTENTS

HYDROSTATIC PRESSURE TESTS ON THIN RECTANGULAR DIAPHRAGMS 21 INCHES BY 13 1/2 INCHES

by

John W. Day

ABSTRACT

Hydrostatic-pressure tests of thin rectangular diaphragms 21 inches by 13 1/2 inches were conducted as a phase of a comprehensive underwater-explosion research program. These tests, which were originally planned as pilot tests for the development of experimental techniques and procedures to be used in testing rectangular diaphragms 7 feet by 4 1/2 feet, were expanded to include laminated diaphragms and diaphragms with various types of stiffeners as well as unstiffened diaphragms. Thus the tests served not only to indicate the techniques and procedures to be used in testing larger diaphragms but also to provide a comparison of unstiffened, stiffened, and laminated diaphragms and to check a theory for rectangular diaphragms under hydrostatic pressure which had been developed previously at the David Taylor Model Basin.

Data such as profiles of deflected diaphragms, curves of center deflection against pressure, thickness, horizontal displacement, volume of displacement of the deflected diaphragms, and energy absorbed were obtained for each of the thirty-six diaphragms tested. Because of the large volume of these data only sample results are presented in this report.

The unstiffened rectangular diaphragms in which the edge bending strains were not excessive absorbed more energy per pound of material before rupture than did the laminated or stiffened diaphragms.

INTRODUCTION

As part of the Bureau of Ships' underwater-explosion research program, static tests of 4 1/2-foot by 7-foot rectangular diaphragms were planned to supplement explosion tests of similar diaphragms which were to be conducted at the Norfolk Naval Shipyard. After the preliminary plans for the static testing rig had been studied, the Taylor Model Basin recommended[1] that tests on a reduced scale be conducted first to gain experience which would be beneficial in the construction and operation of the large-scale testing rig. To carry out this proposal, which was approved by the Bureau of Ships,[2] the

[1]All references are listed on page 42 of this report.

Taylor Model Basin designed and built an apparatus for testing 21-inch by 13 1/2-inch diaphragms. After eight unstiffened diaphragms had been tested under hydrostatic pressure, the program was expanded to include laminated diaphragms and diaphragms with various types of stiffeners. In all, thirty-six diaphragms were tested. For each of these diaphragms data such as profiles of the deflected diaphragms, curves of center deflection against pressure, thickness, horizontal displacement, volume of displacement of the deflected diaphragm, and energy absorbed were measured or computed.

In this report the technique for testing small rectangular diaphragms is described, sample results are presented, and the experimental results are compared with the theory of Reference 3. Data on all the thirty-six diaphragms were recorded and plotted but, because of the space and time required for publication, only selected samples of these data are reproduced in this report. The remaining data have been compiled into an Addendum to this report. This is on file in the Reports Section of the Taylor Model Basin and is available for study by anyone interested in the detailed results.

TEST SETUP AND PROCEDURE

The assembly used to test small rectangular diaphragms under hydrostatic pressure consists essentially of three heavy plates, the outer two of which are clamping frames bolted together as shown in Figure 1. A diaphragm is fillet-welded to each side of the middle plate, as shown in Figure 2. The function of the middle plate is to prevent inward movement of the diaphragm edges while the diaphragms are being deflected by hydrostatic pressure. Because the deflecting diaphragms cause compressive stresses in the middle plate, that plate is called the compression plate. Four large holes in this plate provide access for the water between the diaphragms. The two clamping frames furnish support to the edges of the diaphragms as it was desired to promote failures at locations other than the edge welds.

For each test two diaphragms of equal thickness are cut to the shape shown in Figure 2, and a doubler strip is fillet-welded around the edge of each diaphragm on the pressure side. One diaphragm is then fillet-welded to each side of the compression plate, the weld bead covering both doubler and diaphragm; see inset in Figure 1 and the photograph of Figure 2. The cavities thus formed between the diaphragms and the compression plate and the four large holes in the compression plate represent the volume occupied by the pressure medium. The compression-plate assembly is then bolted between the clamping frames. Spacers, equal in thickness to the combined thickness of the diaphragm and doubler, are placed between the clamping frames and compression plate at the outer edges to prevent bending of the frame. The

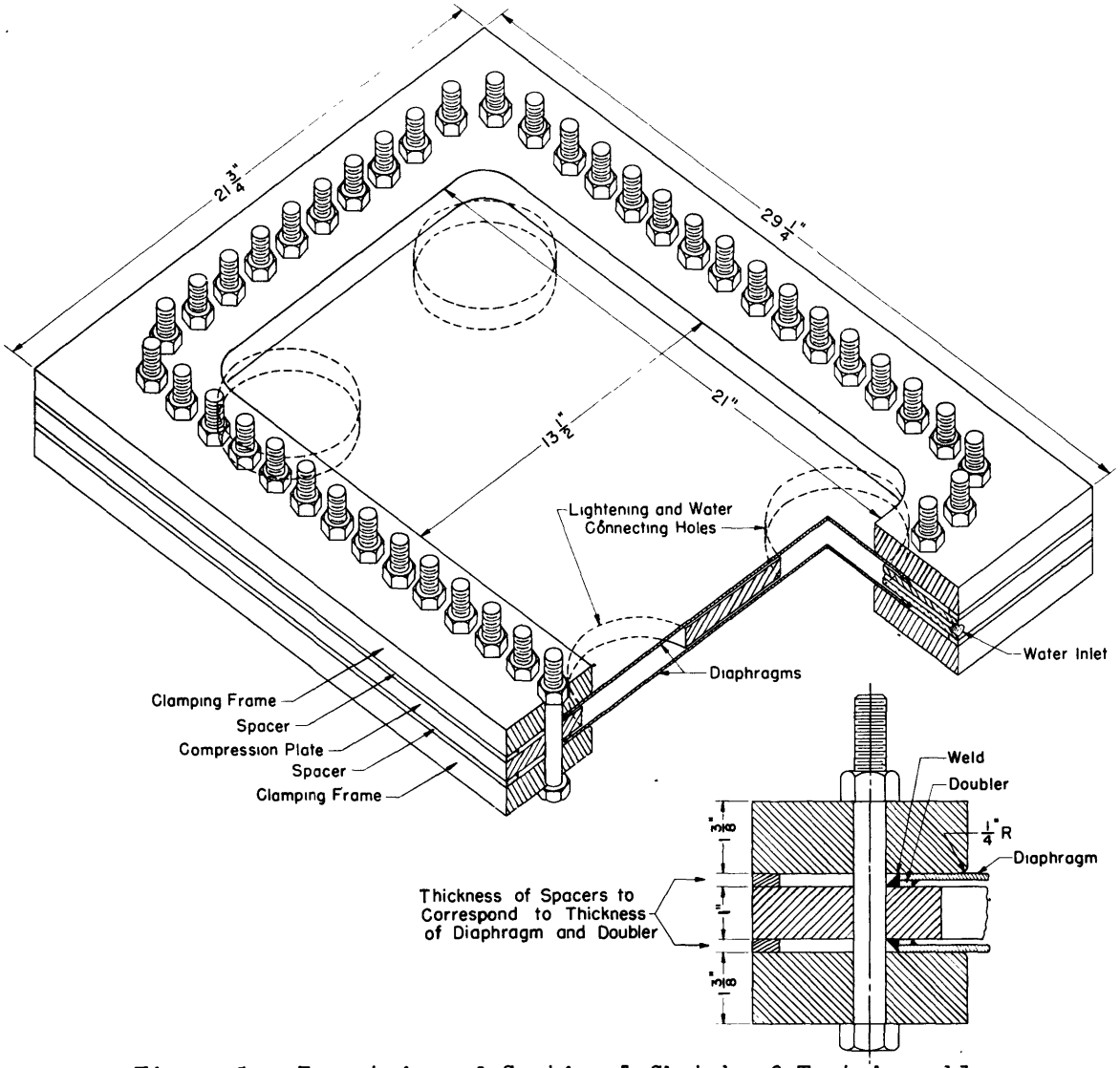

Figure 1 - Isometric and Sectional Sketch of Test Assembly

composite assembly is then connected to a hydraulic circuit at the water inlet shown in Figure 1. All air trapped between the diaphragms can be bled out through an outlet provided with a screw plug. As hydraulic pressure is applied, the diaphragms deflect through the opening in the clamping frame. The inner edges of the clamping frames are rounded with a 1/4-inch radius to reduce the bending and shearing stresses in the diaphragms as they deflect.

The outside surfaces of the diaphragms are sand-blasted to free them from mill scale and rust in order to ensure a smooth surface for measurements. These surfaces are then coated with optical-black lacquer, on which a grid is inscribed on both diaphragms to indicate measuring stations (Figure 3). The additional grids near the rim permitted the obtaining of more data near the

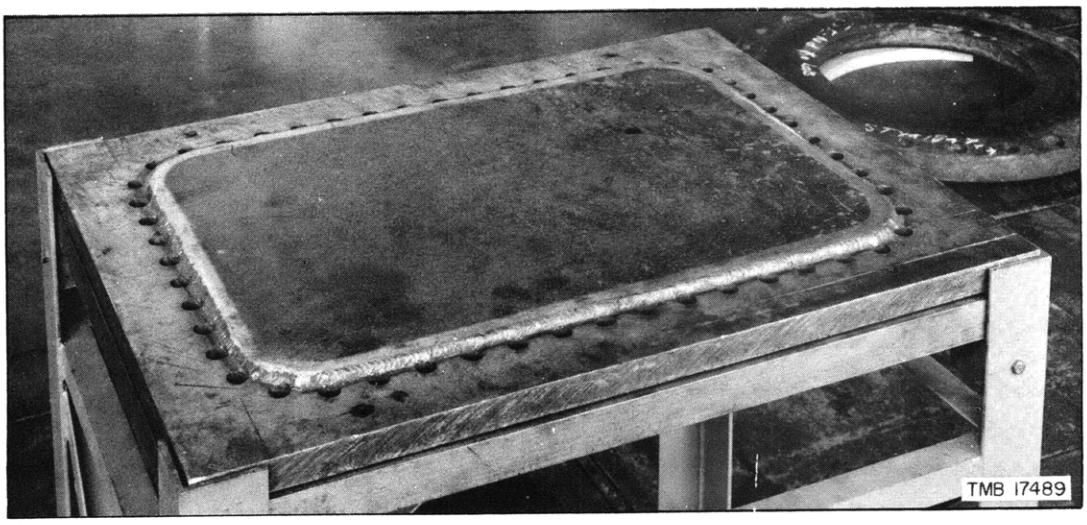

Figure 2 - Compression-Plate Assembly

The shape of the test diaphragm and the manner in which the diaphragm is welded to the heavy compression plate are shown here. A similar diaphragm is welded to the reverse side of the compression plate.

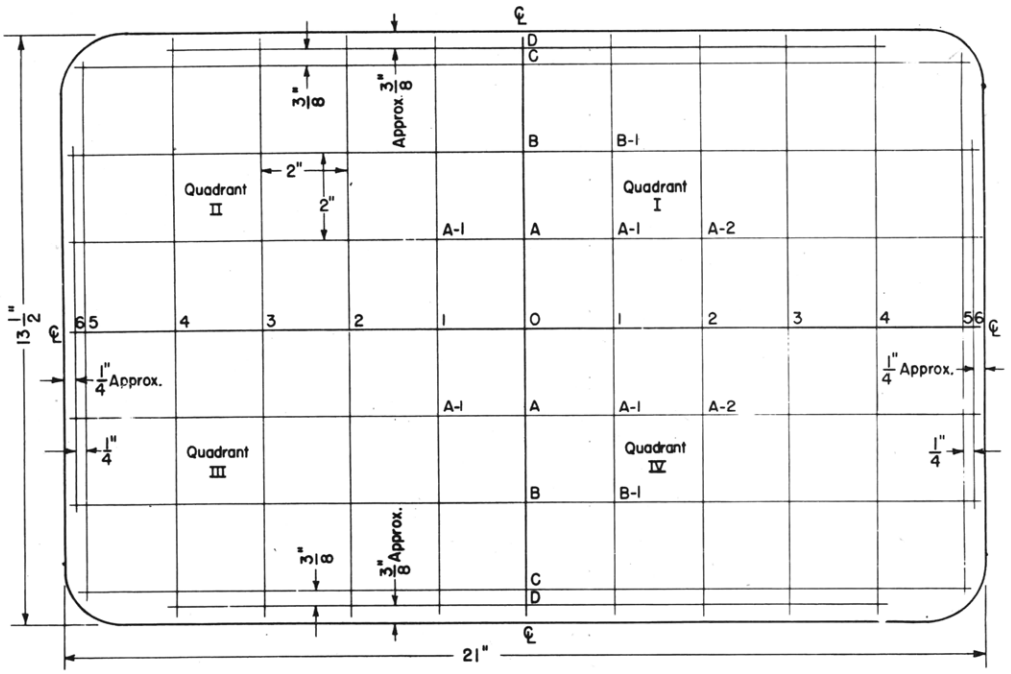

Figure 3 - Grid Layout on Unstiffened Rectangular Diaphragms

diaphragm edges where higher strains were encountered. The grid intersections were designated symmetrically in each quadrant as shown in Figure 3. Measuring stations on the stiffened diaphragms were located at 1- or 2-inch intervals along the stiffeners and, on some diaphragms without longitudinal stiffeners, along the longitudinal centerline of the diaphragm.

After the clamping frames and compression plate have been bolted together, the measuring rig shown in Figure 4 is placed in position. The measuring fixtures are held on the clamping frame by their own weight. The gantry slides along the bearing bars to provide movement of the pointer across the width of the diaphragm. The carriage slides along the gantry bars to provide motion of the pointer over the length of the diaphragm. The pointer slides in a vertical direction through the bushing in the carriage, so that the vertical deflection of the diaphragm can be measured.

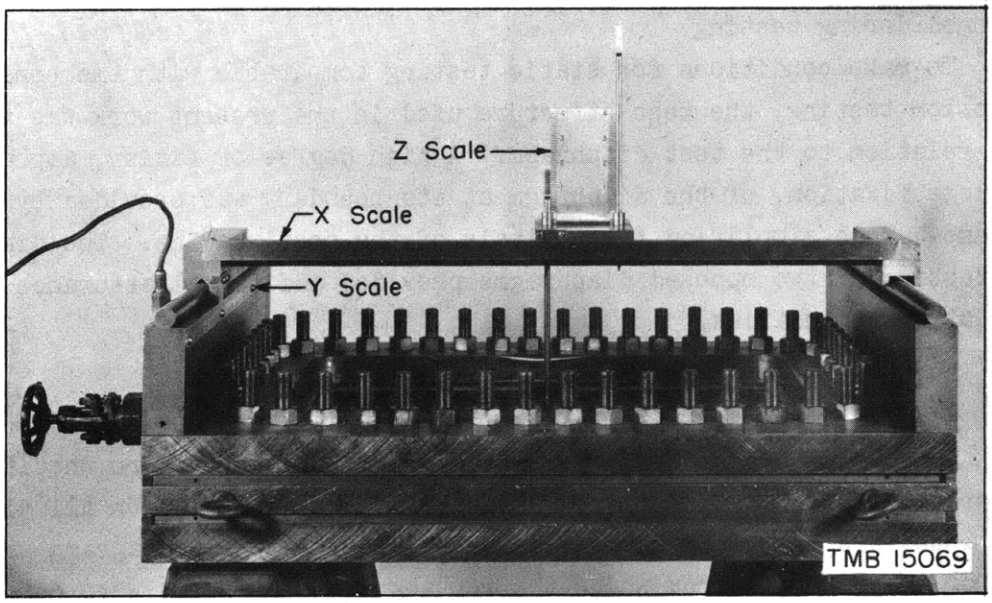

Figure 4 - Measuring Rig Mounted on Test Assembly

In actual testing, pressure was applied to the diaphragms in increments. At each pressure, displacements of each grid station on the diaphragm were measured in three directions as follows:

1. Parallel to the original plane of the diaphragm in a longitudinal direction, designated as x in Figure 4.

2. Parallel to the original plane in a transverse direction, designated as y.

3. Perpendicular to the original plane, designated as z.

After complete data had been taken on the upper diaphragm, termed "obverse" for convenience in identification, the assembly was turned over and data were taken on the "reverse" diaphragm. The pressures were increased by steps until the weaker diaphragm ruptured.

The strains in the diaphragms were computed from the displacements instead of being measured by the usual strain-gage method, for reasons stated under the heading "Test Results and Discussion."

For the first 8 diaphragms, P-1 to P-4, the volumes displaced by the deflected diaphragms were computed from the profile curves of the diaphragms for each pressure step. The computed final volumes were later checked by metering water into the distorted diaphragms until they were filled. The volumes of the remaining 28 diaphragms were measured by the amount of water pumped in deflecting the diaphragms. The final thicknesses of the diaphragms were measured at each grid station to determine the amount the diaphragms had been thinned during testing.

To make conditions for static testing comparable with the conditions for explosion testing, the test structure used in the present work was very heavy in relation to the test diaphragm. A high degree of fixity, approaching complete fixation, of the diaphragm at its boundary was provided by the heavy frame. This simplified the analysis of the test results. The simultaneous testing of two opposed diaphragms provided additional assurance of fixation at the boundaries.

DIAPHRAGMS

Thirty-six diaphragms were tested; of these twelve were unstiffened, twenty were stiffened, and four were laminated. Physical data on all diaphragms tested are listed in Table 1. Tensile stress-strain diagrams were plotted for the material from which the rectangular diaphragms were cut. The diagrams are not included in this report, but are included in the Addendum (see page 2).

UNSTIFFENED AND LAMINATED DIAPHRAGMS

Of the twelve unstiffened diaphragms four had a nominal thickness of 1/4 inch, six had a nominal thickness of 1/8 inch, and two had a nominal thickness of 1/16 inch. Two diaphragms were composed of two 1/8-inch laminae, and two of two 1/16-inch laminae.

TABLE 1

Physical Data on Rectangular Diaphragms

Diaphragm P for Pilot, T for Tee, S for Strap.	Original Thickness of Diaphragm inches	Weight of One Diaphragm pounds	Ultimate Strength of Diaphragm Material psi	Remarks
P-1, Obverse	0.249			Unstiffened
P-1, Reverse	0.250			Unstiffened
P-2, Obverse	0.247			Unstiffened
P-2, Reverse	0.244	19.66		Unstiffened
P-3, Obverse	0.122		70,700	Unstiffened
P-3, Reverse	0.119	9.52		Unstiffened
P-4, Obverse	0.104		46,100	Unstiffened
P-4, Reverse	0.106			Unstiffened
P-5, Obverse	0.134	10.72	41,800	Two laminae
P-5, Reverse	0.134			Two laminae
P-6, Obverse	0.068		41,800	Unstiffened
P-6, Reverse	0.068			Unstiffened
P-7, Obverse	0.248	19.84	66,600	Two laminae
P-7, Reverse	0.248			Two laminae
P-8, Obverse	0.119		61,000	Unstiffened
P-8, Reverse	0.113	9.04		Unstiffened
PS-1, Obverse PS-1, Reverse	0.129	10.32	62,300	Unwelded longitudinal and transverse strap stiffener weighing 1.87 lb
PS-2, Obverse PS-2, Reverse	0.133	10.63		Welded longitudinal and transverse strap stiffener weighing 2.06 lb
PS-3, Obverse PS-3, Reverse	0.128	10.24	67,300	Welded longitudinal and transverse stiffener weighing 1.99 lb
PS-4, Obverse PS-4, Reverse	0.127	10.16	53,500	Unwelded transverse strap stiffener weighing 1.82 lb
PS-5, Obverse PS-5, Reverse	0.119	8.72	61,200	Welded longitudinal and transverse strap stiffener weighing 1.86 lb
PS-6, Obverse PS-6, Reverse	0.049	3.92	69,300	Unwelded transverse bar stiffener weighing 1.40 lb
PS-7, Obverse PS-7, Reverse	0.048	3.84	55,650	Unwelded transverse strap stiffener weighing 1.40 lb
PT-1, Obverse PT-1, Reverse	0.124	9.92		Unwelded longitudinal and transverse tee stiffener weighing 1.92 lb
PT-2, Obverse PT-2, Reverse	0.129 0.124	10.32 9.92	58,900	Welded longitudinal and transverse tee stiffener, weighing 2.07 lb
PT-3, Obverse PT-3, Reverse	0.124	9.92	49,300	Welded longitudinal and transverse tee stiffener weighing 7.98 lb

*All diaphragms and stiffeners were made of medium steel except Diaphragms P-4 which were made of furniture steel.

STIFFENED DIAPHRAGMS

Various types of stiffeners, such as straps, tees, and bars, were used on the stiffened diaphragms. Simplified sketches of the stiffened diaphragms are shown in Figure 5.

Diaphragms PS-1 had longitudinal and transverse unwelded strap stiffeners; Diaphragms PS-2, PS-3, and PS-5 had similar stiffeners which were welded to the diaphragms. The dimensions of the straps are indicated in Figures 5a and 5b.

Diaphragms PS-4 had three transverse unwelded strap stiffeners, and a longitudinal partial strap as shown in Figure 5c.

Simple unwelded transverse strap stiffeners (Figures 5d and 5e) were used on Diaphragms PS-6 and PS-7.

Diaphragms PT-1, PT-2, and PT-3 were stiffened by means of tee stiffeners;see Figures 5f and 5g. For Diaphragms PT-1 the stiffeners were welded to each other but not to the diaphragms. On PT-2 and PT-3 the stiffeners were welded to the diaphragms also.

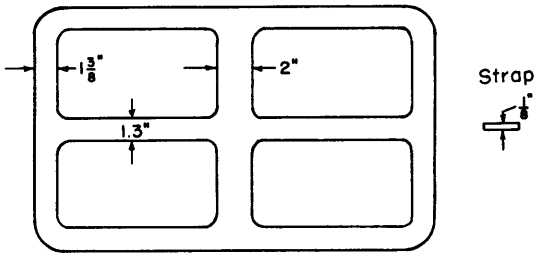

Figure 5a - Diaphragms PS-1

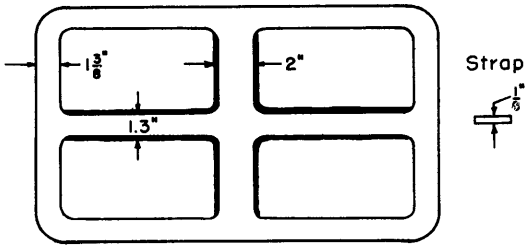

Figure 5b - Diaphragms PS-2, PS-3, and PS-5

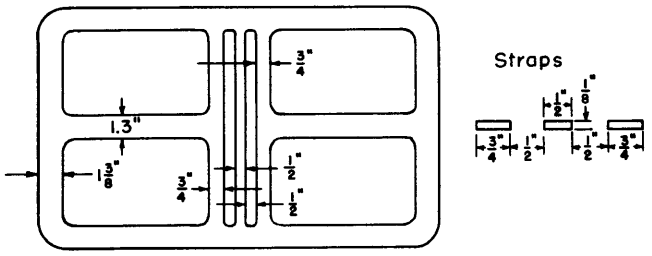

Figure 5c - Diaphragms PS-4

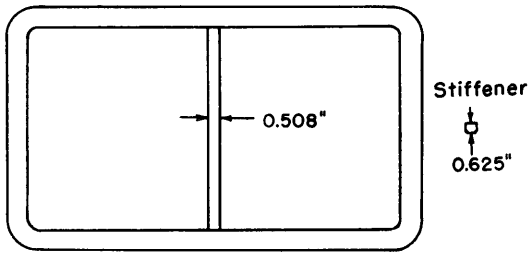

Figure 5i - Diaphragms PS-6

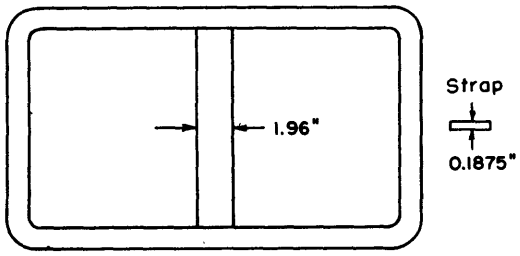

Figure 5e - Diaphragms PS-7

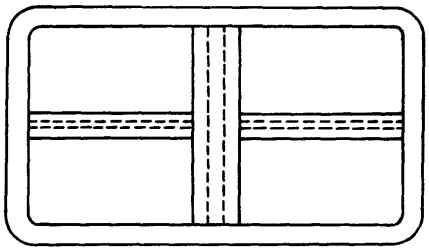

Figure 5f - Diaphragms PT-1, PT-2, and PT-3

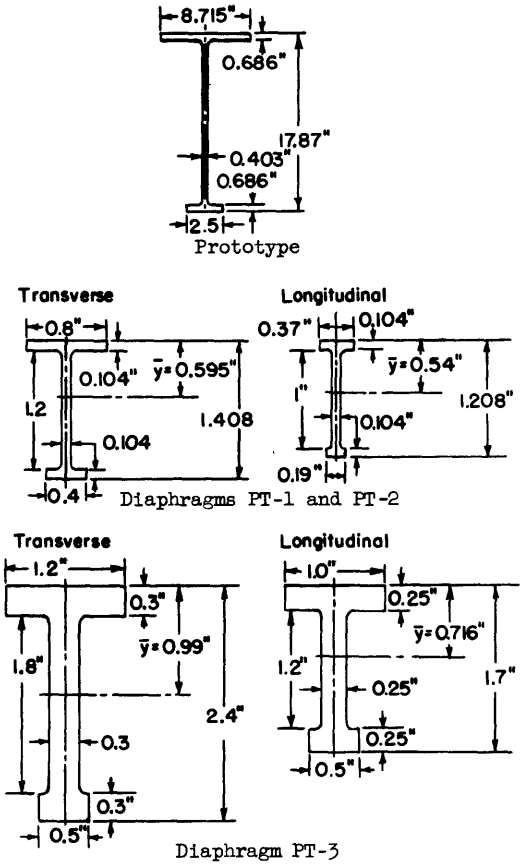

Figure 5g - Sketch of Stiffener Sections

Figure 5 - Dimensions of Diaphragms and Details of Stiffeners

TEST RESULTS AND DISCUSSION

A summary of the measured and computed results of the hydrostatic tests is given in Tables 2, 3, and 4. The detailed results are not presented in this report because of their bulk. Sample curves are reproduced here; similar curves for all other diaphragms tested are available for reference at the Taylor Model Basin.

Much of the text of this section might properly have been placed under the heading "Test Setup and Procedure," but was placed under "Test Results and Discussion" to facilitate possible use of the information of this report in further development of theory or as a basis for continued research.

MEASUREMENTS OF DISPLACEMENTS

Displacements of points on the diaphragms were measured in three planes perpendicular to each other, as indicated in Figure 4. These displacements were determined for each increment of pressure at each of the grid intersections. The measurements of displacements perpendicular to the original plane of the test diaphragm are accurate to within 0.005 inch. Measurements of the displacements parallel to the original plane of the diaphragm are accurate to plus or minus 0.01 inch.

The deflections of points along the major and minor axes of the diaphragms were plotted for each increment of pressure. Typical axial profiles of unstiffened and stiffened diaphragms are shown in Figure 6. Pressure readings were taken after the diaphragms had been subjected to a given pressure long enough for a stable condition to develop through plastic readjustments in the metal. The pressure was then released, and readings were again taken. Hence the difference between any deflection curve for a given pressure and the subsequent deflection curve for atmospheric pressure represents the elastic deflection of the material.

Comparison of the curves of Figure 6 shows the effect of axial stiffeners on the shape of the profiles. The profiles of the unstiffened diaphragms approximate parabolas. The longitudinal and transverse axial strap stiffeners produced a profile the shape of which approximated an oblate parabola. The effect of the longitudinal axial stiffener (not illustrated) is, however, observable only at low pressures because of the higher restraint of the shorter transverse axis as high pressures are approached. The presence of a transverse axial stiffener produced a "saddling" effect in the longitudinal profile of the diaphragm; see Figure 6d.

TABLE 2

Results of Hydrostatic Tests on Rectangular Diaphragms

Diaphragm	Final Center Deflection Z_o inches	Rupture Pressure psi	Ratio of Equivalent Radius* to Thickness	Final Measured Volume cubic inches	Total Energy Absorbed $W = \int pdV$ inch-kips	Energy Absorbed per Pound of Weight inch-kips per pound	Location and Type of Failure
P-1, Obverse	1.50	890	38.9	210.9	93.8	4.68	Center of long edge. Fillet weld toe.
P-1, Reverse	1.46		38.8	204.4	90.9	4.31	
P-2, Obverse	1.65	1200	39.2	229.2	137.5	7.01	Center of long edge. Weld.
P-2, Reverse	1.72	1200	39.7	248.8	149.4	7.61	Center of long edge. Incipient plate failure.
P-3, Obverse	2.60		79.5	383.5	181.7	18.50	
P-3, Reverse	2.54	950	81.5	386.8	183.7	19.17	Center of long edge.
P-4, Obverse	2.76	600	93.3	414.8	124.4	14.87	Center of long edge.
P-4, Reverse	2.69		91.5	386.9	116.2	13.61	
P-5, Obverse	2.44	700	72.5	379.1	114.2	10.65	Center of long edge. Tear in plate
P-5, Reverse	2.45			380.6	114.6	10.70	
P-6, Obverse	3.12		142.6	473.0	93.1	17.37	
P-6, Reverse	3.33	435		504.8	99.0	18.46	About 1 inch from edge in long side of plate
P-7, Obverse	1.77		39.1	267.4	153.4	7.73	
P-7, Reverse	1.82	1250		274.9	158.3	7.97	Center of long edge. Weld throat.
P-8, Obverse	2.78		83.5	411.5	174.0	18.75	
P-8, Reverse	2.77	920		409.3	173.6	18.71	Center of long edge. Plate.
PS-1, Obverse	2.29		75.2	348.8	191.9	15.74	
PS-1, Reverse	2.23	1100	75.2	339.7	186.7	15.31	Long edge of diaphragm at edge of unwelded strap structure.
PS-2, Obverse	2.26	850	72.9	358.9	152.5	12.03	Long edge of diaphragm at edge of unwelded strap structure.
PS-2, Reverse	2.24		72.9	355.7	151.0	11.90	
PS-3, Obverse	1.98		75.8	312.5	167.9	13.73	
PS-3, Reverse	1.98	1075	75.8	312.5	167.9	13.73	Crack in plate, weld, stiffener-end transverse stiffener.
PS-4, Obverse	2.59	900	76.4	379.5	170.8	14.25	Long edge of diaphragm at stiffener.
PS-4, Reverse	2.37		76.4	353.4	159.0	13.27	
PS-5, Obverse	1.60	675	81.5	241.0	81.4	7.69	Transverse strap stiffener near longitudinal stiffener. Blow hole in weld.
PS-5, Reverse	1.56		81.5	235.4	79.5	7.52	
PS-6, Obverse	1.21	270	198.0	238.1	32.2	6.04	Long edge of diaphragm, 3 inches from stiffener.
PS-6, Reverse	1.20		198.0	236.2	31.9	6.00	
PS-7, Obverse	1.45		202.0	266.0	44.6	8.50	
PS-7, Reverse	1.47	335	202.0	270.5	45.3	8.64	Long edge of diaphragm under stiffener.
PT-1, Obverse	1.86	750	78.2	311.2	116.6	9.84	Web of longitudinal stiffener near end welds at frame.
PT-1, Reverse	1.85		78.2	295.3	110.7	9.36	
PT-2, Obverse	1.06		75.2	175.0	39.4	3.18	
PT-2, Reverse	1.09	450	78.2	180.0	40.5	3.38	Frame end of transverse stiffener. Weld.
PT-3, Obverse	0.27	385	78.2	78.1	15.03	0.841	
PT-3, Reverse	0.32	385	78.2	92.7	17.85	0.997	Stiffener welds cracked at all locations.

*The equivalent radius a_o is defined by the equation

$$\frac{1}{a_o^2} = \frac{16}{45}\left(\frac{1}{a_1^2} + \frac{1}{a_2^2}\right)$$

TABLE 3

Comparisons of Test Results of Single and Double Unstiffened Diaphragms

Diaphragm	Original Total Thickness inches	Construction and Lamination	Final Center Deflection inches	Rupture Pressure pounds	Final Volume cubic inches	Diaphragm Weight pounds	Energy Absorbed in. kips/lb
P-2	0.244	Single	1.72	1200	248.8	19.66	7.61
P-7	0.248	Double*	1.82	1250	274.9	19.84	7.97
P-3	0.119	Single	2.54	950	386.8	9.52	19.17
P-8	0.113	Single	2.77	920	409.3	9.04	18.71
P-5	0.134	Double	2.44	700	379.1	10.72	10.65

*The double laminated diaphragms are made of two sheets in contact.

Curves of center deflection plotted against pressure are shown in Figure 7. The points on the upper curves represent deflections of the centers of the diaphragms at the given pressures. The points on the curves of permanent set represent the deflections of the diaphragms after the pressure had been reduced from the pressure of the corresponding point on the upper deflection curve to the pressure indicated on the lower curve. For the range of deflections common to both rectangular and circular diaphragms, these curves are similar in shape to those plotted for the 20-inch circular diaphragms and shown in Figure 12, page 14, of Reference 4. Because of geometrical differences the center deflection of the rectangular diaphragms at rupture is approximately half that of the 20-inch circular diaphragm. The 1/4-inch radius of the rim of the clamping frame of the rectangular diaphragm, as contrasted with the 1/2-inch radius of that of the circular diaphragm, produces higher bending stresses in the edge of the rectangular diaphragm and promotes rupture at a lower center deflection.

Some of the curves of center deflection against pressure for the stiffened diaphragms are somewhat irregular (Figure 7d). A possible explanation for this would be a local mal-distribution of strain caused by heterogeneous conditions in the metal of the structure brought about by the presence of weld metal and the attendant effects of the welding heat on the metallurgical characteristics of the metal of the diaphragm and stiffeners. It could also be attributed to a local buckling or rotation due to lack of symmetry of the stiffeners of the tee-stiffened diaphragms.

Figure 7c will be found of interest as the additional points taken at low pressures reveal the deflection characteristics of a diaphragm in the elastic region and in the very low plastic region.

The displacement parallel to the original plane of the diaphragm of points on the major and minor axes of the diaphragms are plotted in Figure 8. In Sketch 8a the point P_o represents a grid station on the originally flat diaphragm. As the diaphragm deflects, the point P_o moves over the curved path to the point P. The quantities x, in the case of the long axis, and y, in the case of the short axis, represent the distance of the grid point from the center point of the originally flat diaphragm. The quantities u and v represent the displacements after failure, in the x and y directions respectively, of the point. The graph symbols x represent points on the obverse diaphragm, the symbols + points on the reverse diaphragm. Displacements were taken after the diaphragm ruptured and the pressure was zero.

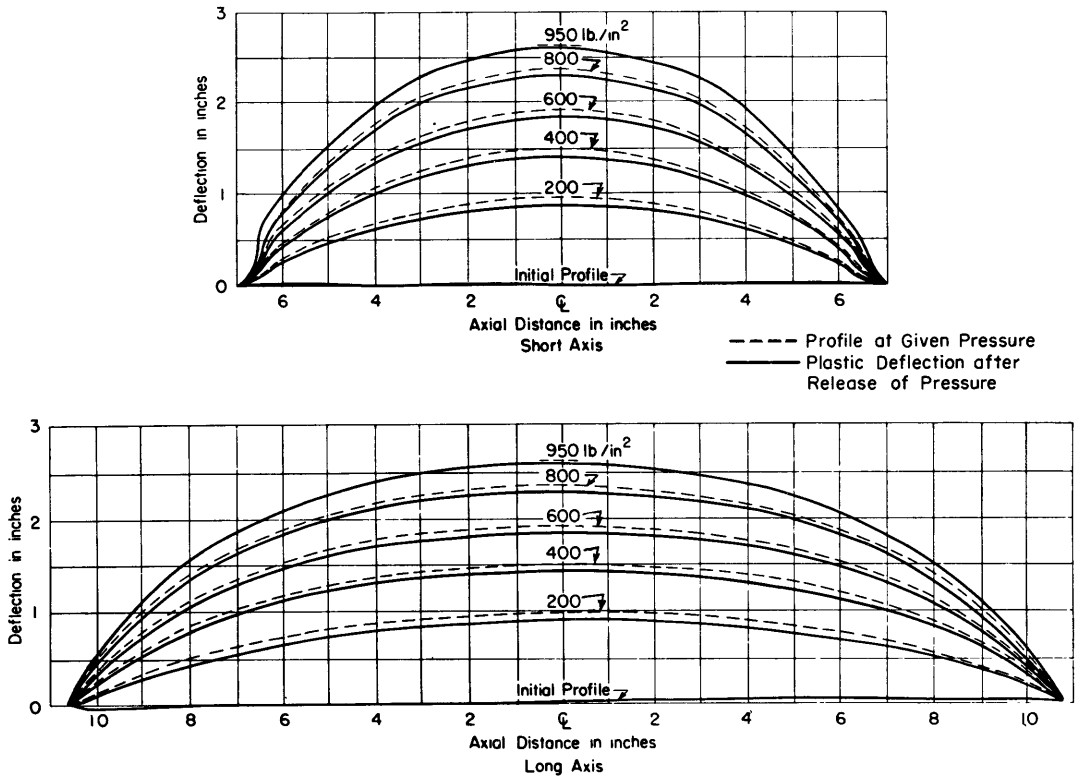

Figure 6a - Profiles of 1/8-Inch Medium-Steel Diaphragm P-3, Obverse

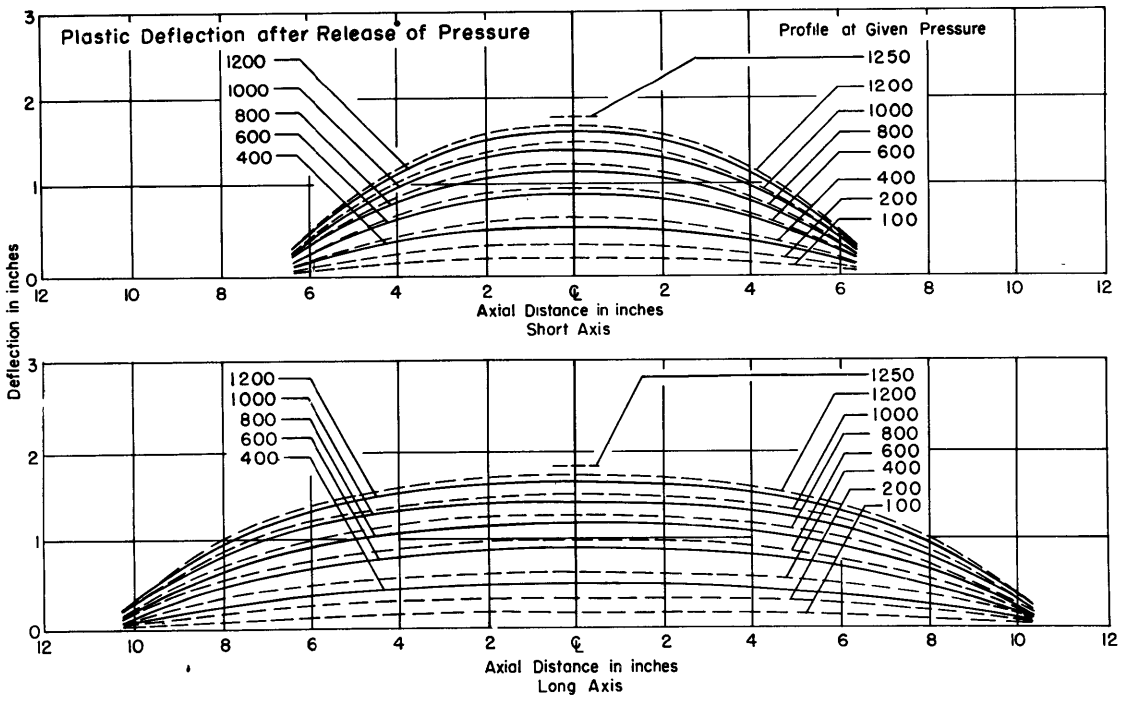

Figure 6b - Profiles of 1/4-Inch Laminated Medium-Steel Diaphragm P-7, Reverse

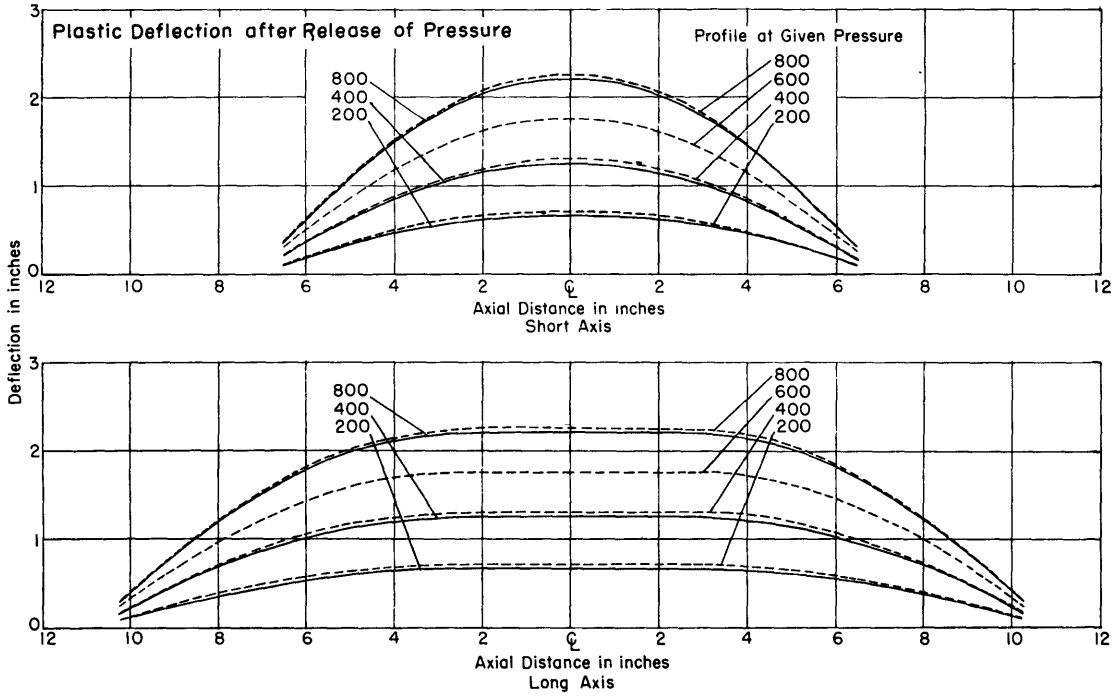

Figure 6c - Profiles of 1/8-Inch Medium-Steel Diaphragm PS-2, Obverse, with Welded Strap Stiffeners on Longitudinal and Transverse Axes

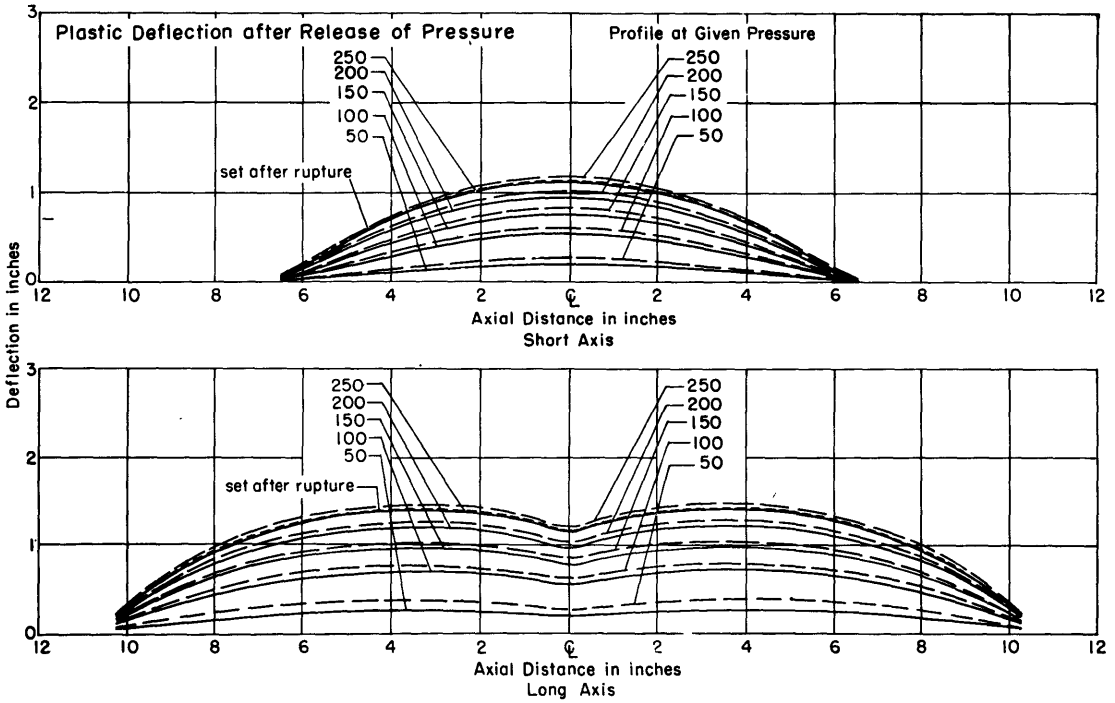

Figure 6d - Profiles of 3/64-Inch Medium Steel Diaphragm PS-6, Reverse with Transverse Bar Stiffener

The long-axis curves were taken on the centerline of the plate surface and show the constricting effect of the stiffener on the plate at the center point.

Figure 6 - Profiles of Diaphragms at Various Pressures Showing the Effect of Stiffeners

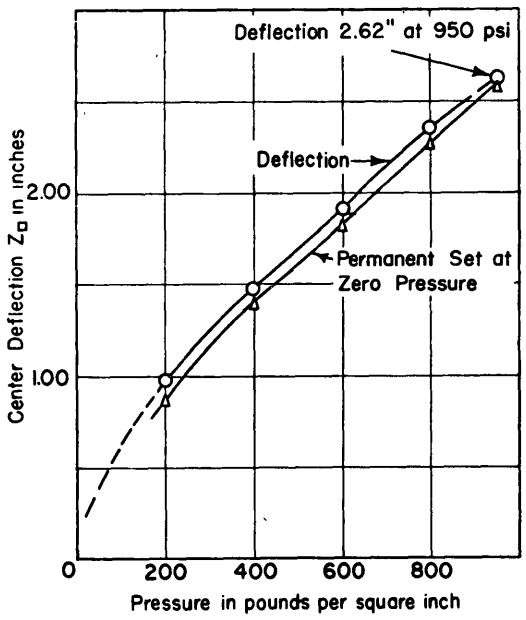

Figure 7a - Center Deflection of 1/8-Inch Medium-Steel Diaphragm P-3, Obverse

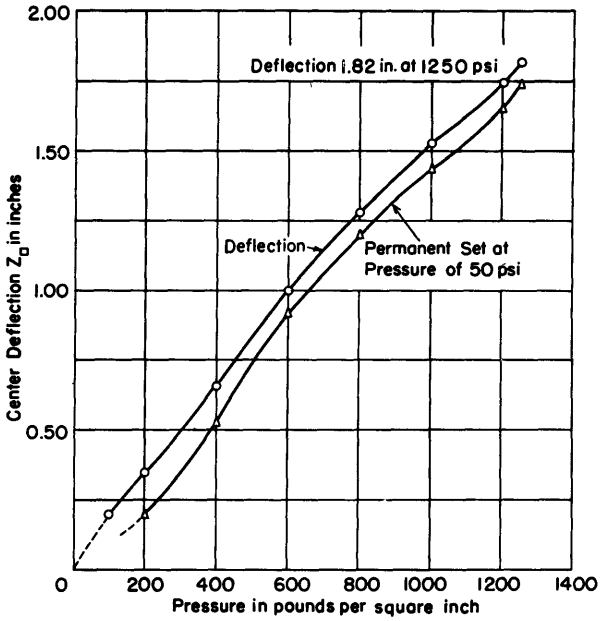

Figure 7b - Center Deflection of 1/4-Inch Laminated Medium-Steel Diaphragm P-7, Reverse

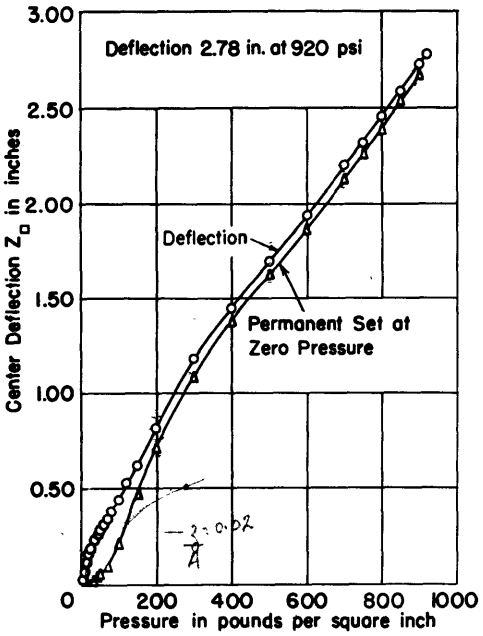

Figure 7c - Center Deflection of 1/8-Inch Medium-Steel Diaphragm P-8, Obverse, Unstiffened

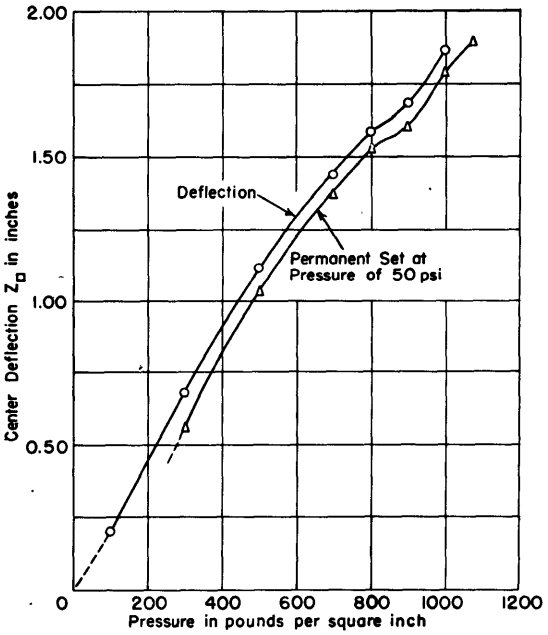

Figure 7d - Center Deflection of 1/8-Inch Medium-Steel Diaphragm PS-3, Obverse, with Welded Strap Stiffeners

Figure 7 - Center Deflection Plotted against Pressure

The upper curve represents the deflection of the diaphragm under pressure. The curve of permanent set represents the deflection of the diaphragm after the pressure was dropped to a lower pressure, which is indicated in each figure.

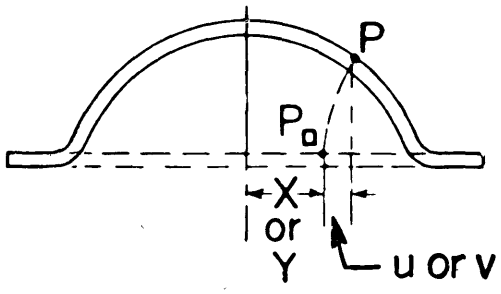

Figure 8a - Diagrammatic Sketch of Axial Displacements of Diaphragms

× - OBVERSE
\+ - REVERSE

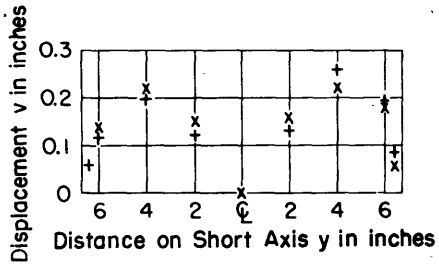

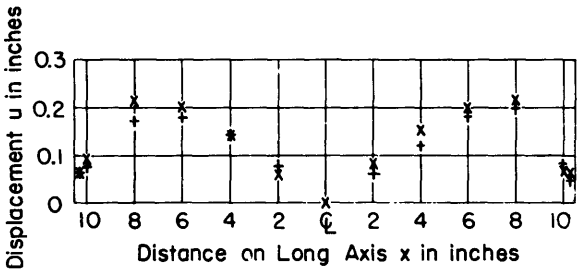

Figure 8b - Axial Displacements After Rupture of 1/8-Inch Medium-Steel Diaphragms P-3

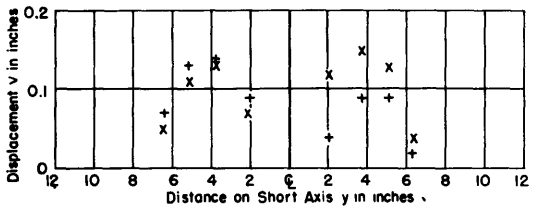

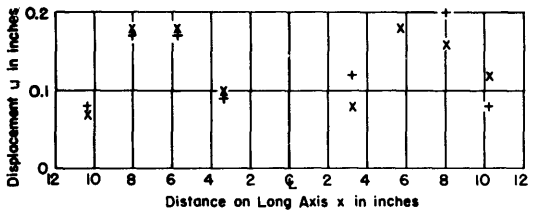

Figure 8c - Axial Displacements After Rupture of 1/8-Inch Medium-Steel Diaphragms PS-2 with Welded Strap Stiffeners

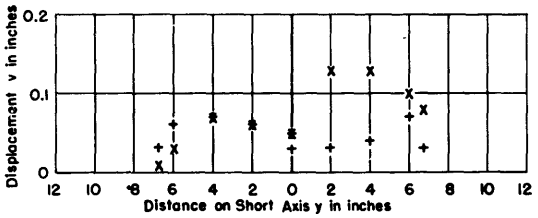

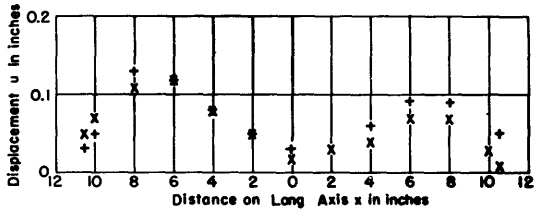

Figure 8d - Axial Displacements After Rupture of 1/4-Inch Laminated Medium-Steel Diaphragms P-7

Figure 8 - Axial Displacements of Stiffened and Unstiffened Diaphragms

TABLE 4

Volume of Displacement and Energy Absorption Data on Unstiffened Rectangular Diaphragms

Diaphragms	Final Measured Volume cubic inches	Computed* Volume cubic inches	Volume Variance percent	Total Energy Absorbed $W = \int pdV$ From Test inch-kips	Approximate Total Energy** Absorbed inch kips	Approximate Energy Variance percent	Energy Absorbed in. kips/lb
P-1, Obverse	210.9	194.8	-7.63	93.8	123.8	32	4.68
P-1, Reverse	204.4	189.6	-7.24	90.8	117.9	30	4.31
P-2, Obverse	229.2	214.5	-6.50	137.5	148.7	8.15	7.01
P-2, Reverse	248.8	223.5	-10.20	149.4	159.4	6.7	7.61
P-3, Obverse	383.5	337.6	-11.97	181.7	182.3	0.3	18.50
P-3, Reverse	386.8	329.8	-14.74	183.7	169.8	-7.6	19.17
P-4, Obverse	414.8	358.4	-13.60	124.4	114.1	-8.3	14.87
P-4, Reverse	386.9	349.3	-9.72	116.2	110.5	-4.9	13.61
P-5, Obverse	379.1	317.0	-16.4	114.2	106.6	-6.65	10.65
P-5, Reverse	380.6	318.5	-16.3	114.6	107.5	-6.20	10.70
P-6, Obverse	473.0	406.0	-14.1	93.1	85.2	-8.49	17.37
P-6, Reverse	504.8	433.0	-14.2	99.0	97.2	-1.82	18.46
P-7, Obverse	267.4	230.0	-14.0	153.4	161.3	4.90	7.73
P-7, Reverse	274.9	236.5	-14.0	158.3	170.5	7.72	7.97
P-8, Obverse	411.5	361.0	-12.3	174.0	170.4	-2.07	18.75
P-8, Reverse	409.3	360.0	-12.0	173.6	169.2	-2.53	18.71

*The computed volume is equivalent to $\frac{16}{9} a_1 a_2 Z_\square$

**The approximate total energy is expressed $W_\square = \frac{64}{45}\left(\frac{a_2}{a_1} + \frac{a_1}{a_2}\right) \sigma_\square h_\square Z_\square^2$

MEASUREMENTS OF STRAIN

Plastic strains of the type encountered in these tests may be as much as 20 percent; consequently the use of the strain-grid method for measuring strains was considered sufficiently accurate, and more accurate strain measurements by other techniques were not included in the tests.

In Figure 9 is shown the grid marked on the test diaphragm in its initial flat state to form 2-inch squares. The values given represent the displacements of the intersection points from their initial positions before testing to their final positions after rupture. The values at the center 0 give the sequence of all other values. Positive values of x and y indicate displacements of a point normal to, and away from, the axes YOY and XOX respectively. Negative values of x and y indicate displacements toward the respective axes. The z values represent the total deflection normal to the initial surface of the diaphragm.

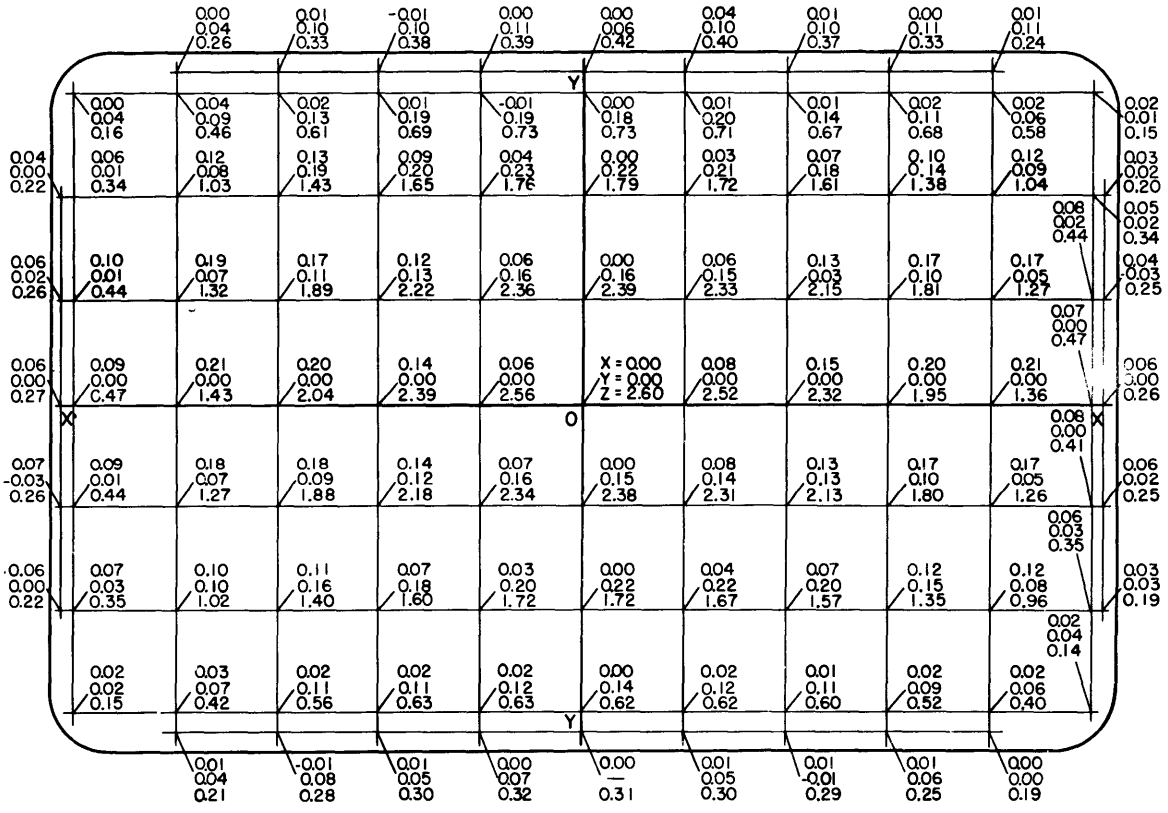

Figure 9 - Grid Measurements of Displacement and Deflection for 1/8-Inch Medium-Steel Diaphragm P-3, Obverse

The total displacements of each grid station were tabulated in diagrams similar to Figure 9 for all diaphragms tested. From the values given in these figures the average strains for successive positions on the major and minor axes of the diaphragms were computed. Figure 10 shows the average strains at 2-inch intervals along the centerlines plotted against center deflections for representative diaphragms. The strains are based on the change in chord length between adjacent grid intersections and are plotted at the midpoint of the initial base length. The strain curves for positions near the edges of a diaphragm may be influenced by bending, which could account for the irregular shapes at such locations. The curves of strain against center deflection for the stiffened diaphragms were so erratic that they have little meaning for comparative purposes and none are reproduced here. This erratic characteristic of the stiffened diaphragms carried over, obviously, to the strain curves plotted against axial distances. Representative curves of strain plotted against axial distance are reproduced in Figures 11, 12, and 13. The longitudinal and transverse average strains at points at 2-inch intervals along the axes are plotted for each pressure increment taken during the test. It will be noted that the curves for the highest pressure show one more strain station than the other curves. The measurement at the additional station represents the total plastic strain at the point where the longitudinal or transverse centerline of the diaphragm passed under the heavy clamping frame of the test assembly. This point was accessible only before the clamping frames were assembled and after they were disassembled; hence only the total plastic strain was obtainable in these areas. These strains were measured point to point without using the measuring rig.

The conformation of the transverse strain curves for the stiffened diaphragms was roughly similar to that of the transverse strain curves for the unstiffened diaphragms. However, at the center of the longitudinal strain curve there was a sharp dip in the strain values resulting from the constraining effect of the transverse strap. The somewhat erratic disposition of the strain curves for the stiffened diaphragms may probably be explained by the possibility of the presence of local strain phenomena resulting from partial intermittent composite action of the stiffeners and the diaphragm in the case of unwelded stiffeners, and of the effect of readjustment of welding strains where the stiffeners were welded to the diaphragm. The constraining effect of the transverse tee stiffener (on diaphragms with longitudinal and transverse tee stiffeners) is more marked, as evidenced by the longitudinal strain curves, than is that of the transverse strap stiffeners on diaphragms with only transverse strap stiffeners. The curves of strain along the transverse tee stiffener (not illustrated) take a shape similar to

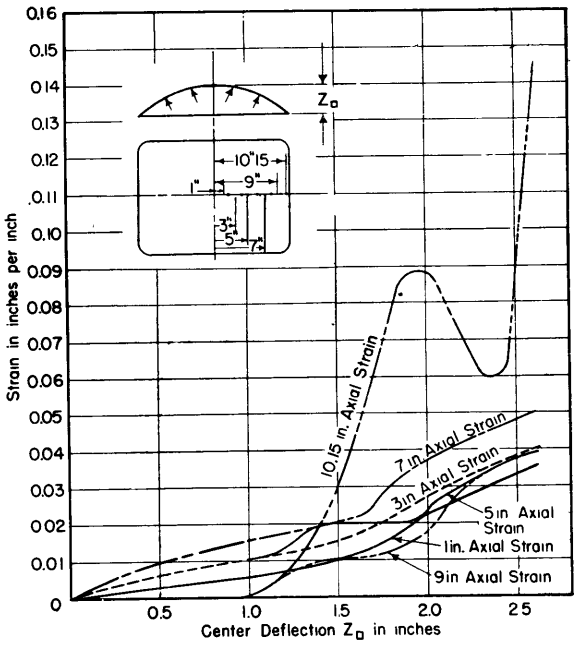

Figure 10a Longitudinal Axial Strain in 1/8-Inch Solid Diaphragm P-3, Obverse

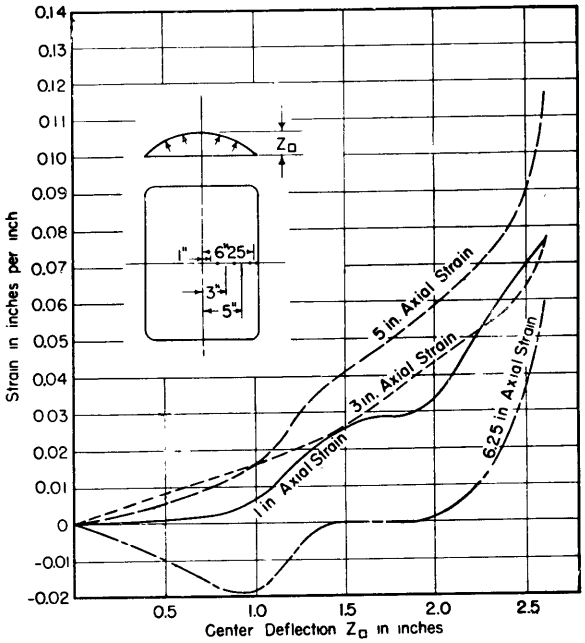

Figure 10b - Transverse Axial Strain in 1/8-Inch Solid Diaphragm P-3, Obverse

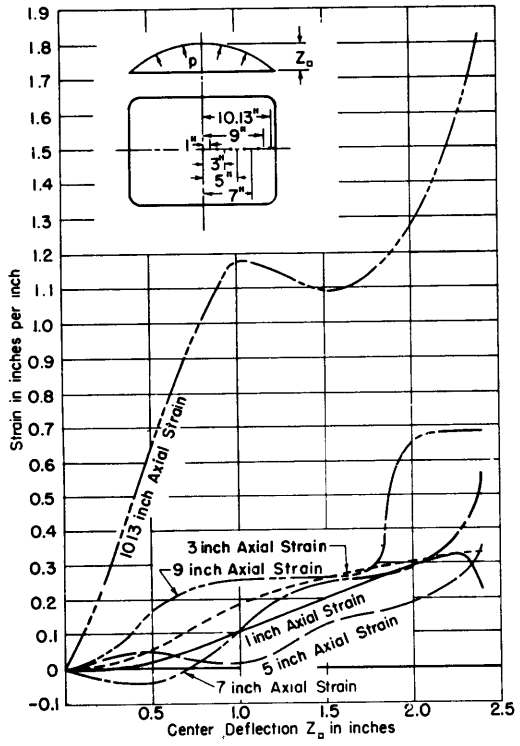

Figure 10c - Longitudinal Axial Strain in 1/8-Inch Laminated Diaphragm P-5, Obverse

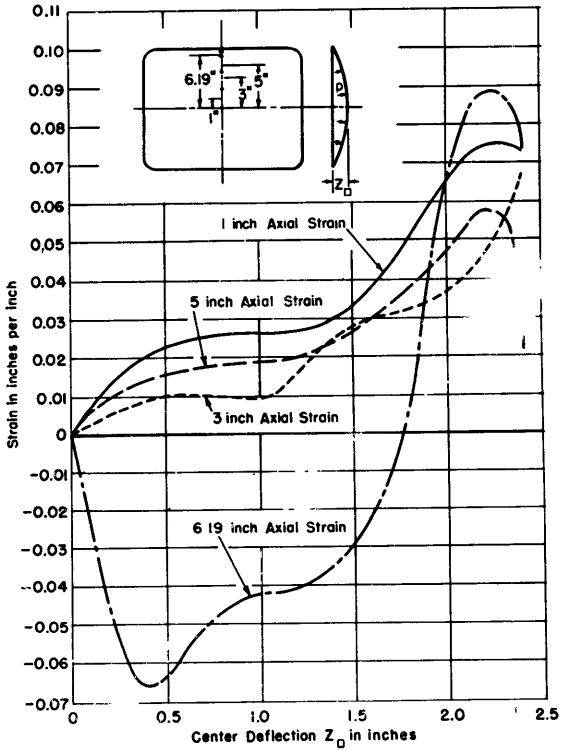

Figure 10d - Transverse Axial Strain in 1/8-Inch Laminated Diaphragm P-5, Obverse

Figure 10 - Longitudinal and Transverse Axial Strains In Two Medium-Steel Diaphragms

Base length for strains is 2 inches except at edges of diaphragms.

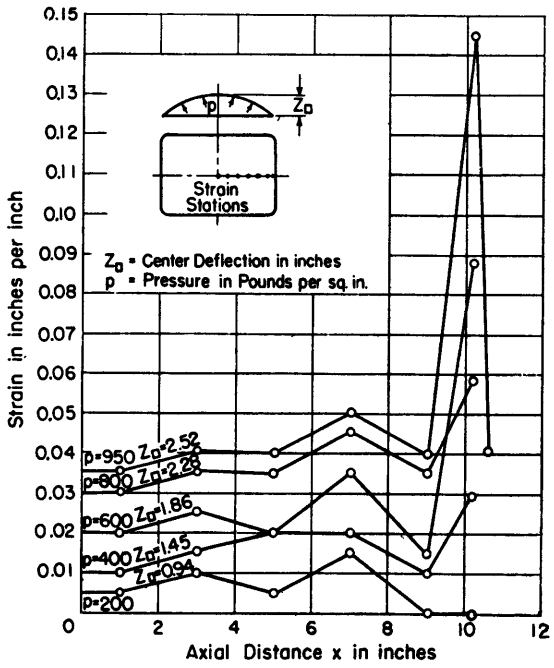

Figure 11a - Longitudinal Strain

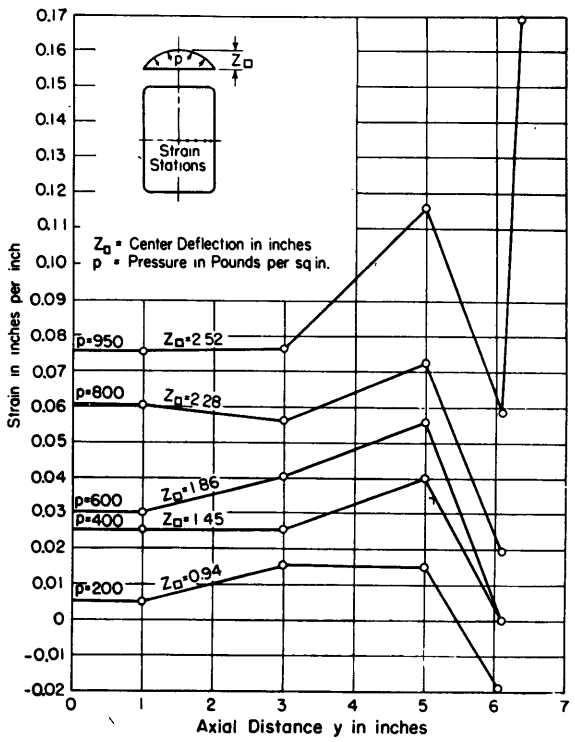

Figure 11b - Transverse Strain

Figure 11 - Strain in 1/8-Inch Medium-Steel Diaphragm P-3, Obverse, Plotted against Axial Distance

The curve for p = 950 psi represents plastic strains only. The remaining curves represent both plastic and elastic strains for the given pressures.

the strain curve of a beam with fixed ends and show little, if any, effect from the longitudinal stiffener. They are also roughly similar in conformation to the strain curves of the 20-inch circular diaphragms shown on pages 27 and 28 of Reference 5.

MEASUREMENTS OF THICKNESS

To determine whether the thickness of the diaphragms decreased systematically from edge to center along the longitudinal and transverse axes, measurements were made at each grid intersection after the diaphragms had been tested and removed from the assembly. A dial-gage micrometer with an accuracy of ± 0.001 inch was used for these measurements. The thicknesses thus measured were plotted for some of the unstiffened diaphragms and some with the stiffeners; sample plots are reproduced here in Figure 14.

The circular diaphragms thinned under hydrostatic pressure in an increasing amount from the edges toward the center;[5] so much so that the difference in thickness of center and of edges was visible. The difference in

final thickness of center and edges of the unstiffened rectangular diaphragms is far less evident, but the center tends to be thinner than the edges. However, in a fixed-ended transverse strap where the strains are essentially uniaxial tensile strains, the thinning of the strap seems to be constant over the length of the strap. The same uniform thinning characteristic also seems to hold along the longitudinal centerline of transversely stiffened Diaphragms PS-6 and PS-7, notwithstanding the fact that the strains are more biaxial.

VOLUME OF DISPLACEMENT BY DEFLECTION OF DIAPHRAGMS

The volume of displacement of a deflected diaphragm may be defined by assuming the diaphragm to be a rectangular membrane held fixed at the edges. The volume constitutes the space between the original plane of the membrane and the dished shape taken by the inside surface of the membrane as a result of the application of hydrostatic pressure.

The volumes of displacement of the deflected diaphragms are shown in relation to the center deflections in Figure 15. These curves represent the volume of liquid pumped between the diaphragms after initial filling of the cavity at atmospheric pressure, terminating when rupture of one diaphragm occurs. The volume change represents the elastic and plastic deflection of the free area of both diaphragms encompassed by the clamping frames. Both diaphragms deflect approximately the same amount until one is ruptured.

The final volumes are those measured after the assembly had ruptured, i.e., the final plotted value represents only the volume at plastic deflection, whereas the remainder of the curve represents the volumes at combined elastic and plastic deflections for the plotted pressure.

The computed final volumes varied 6 percent to 16 percent from the actual measured volumes. The actual measured volumes were obtained to an accuracy of ± 0.5 cubic inch.

ENERGY ABSORBED BY DEFLECTED DIAPHRAGMS

The energy values for the several diaphragms were computed from the volume values and the equation $W = \int p\,dV$, where W is the energy absorbed in inch-pounds, p is the pressure in pounds per square inch, and dV is an increment of volume. The energy curves in Figure 16 were plotted from these values. The energy curves for the stiffened diaphragms were generally similar in shape to those of the unstiffened rectangular diaphragms. When the energy curves of laminated diaphragms were compared with those of single unstiffened diaphragms at the same deflection, it was found that the laminated diaphragms had a greater rate of energy absorption than a single diaphragm of equivalent

thickness. The ratio of the absorption rates of one set of single and laminated diaphragms was the same as for a thicker set of diaphragms. This observation would logically lead to the supposition that a laminated diaphragm would absorb more energy than a single one of equivalent thickness. However this supposition does not necessarily follow as will be shown in a following section.

RUPTURE OF DIAPHRAGMS

Views of ruptures of some of the diaphragms are shown in Figures 17, 18, and 19. All of the unstiffened diaphragms except Diaphragms P-6 ruptured at the middle of a long side of the diaphragm where the diaphragm

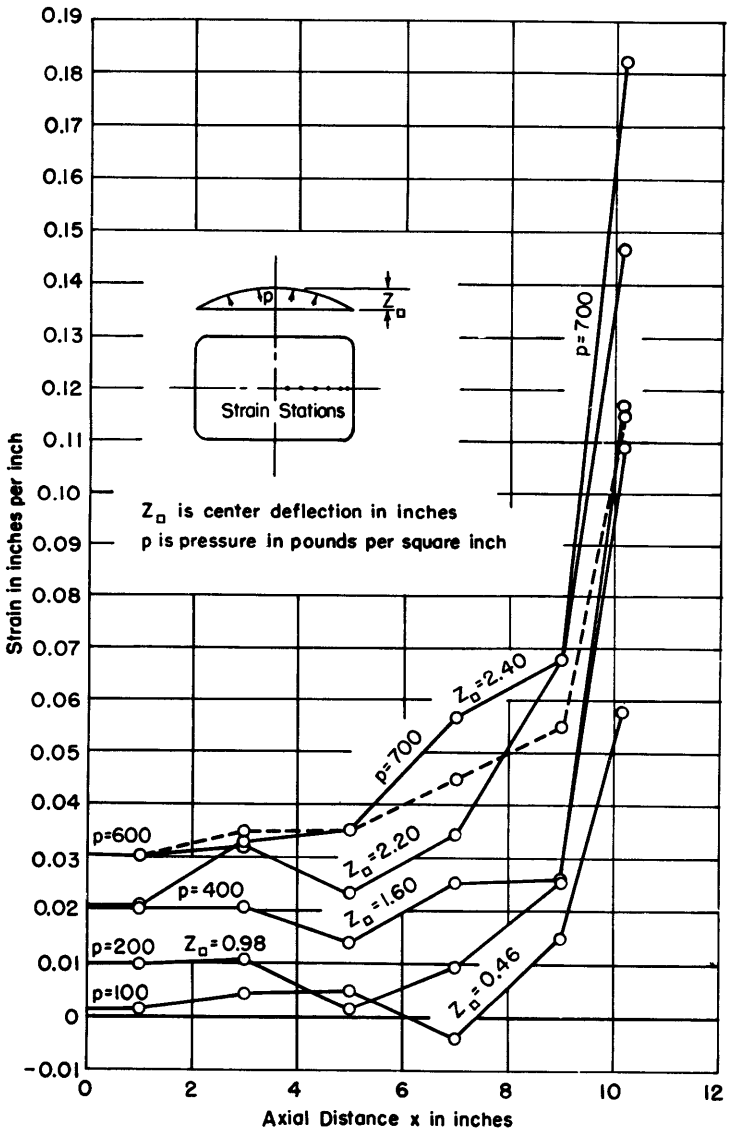

Figure 12a - Longitudinal Strain

bent over the edge of the clamping frame (Figure 17). Rupture of Diaphragms P-6 occurred in the long side 1 1/4 inch from the edge of the diaphragm; see Figure 18. This was an area of high strain in all the unstiffened diaphragms. The reason for this mode of failure in Diaphragms P-6 may have been the high value of the ratio $a_{\square}/h_{\square}$ which minimized the bending strains at the edge of the diaphragm.

Most of the stiffened diaphragms also failed near the center of the long edge. Other types of failure in stiffened diaphragms are shown in Figures 19 and 20.

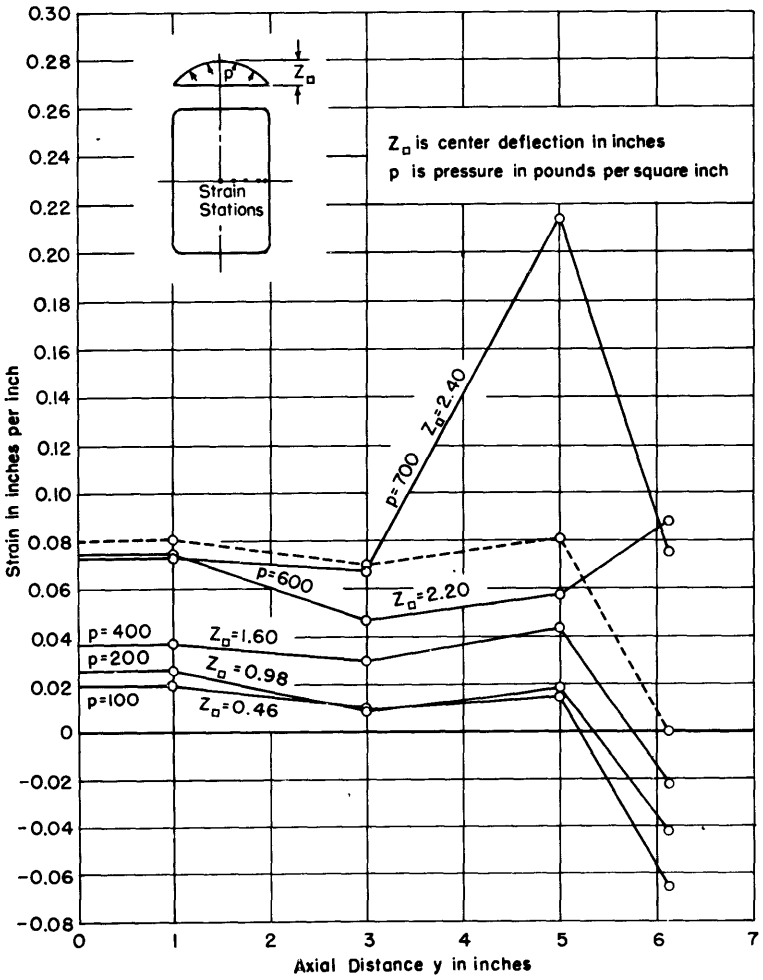

Figure 12b - Transverse Strain

Figure 12 - Strain in 1/8-Inch Laminated Medium Steel Diaphragm P-5, Obverse, Plotted against Axial Distance

The curve for p = 700 psi represents plastic strains only. The remaining labeled curves represent both plastic and elastic strains for the given pressures. The broken-line curve represents the plastic strains computed from elongation measurements made on the diaphragm after it was machined from the compression plate.

COMPARISON OF STIFFENED AND UNSTIFFENED DIAPHRAGMS

The best disposition of a given weight of material, as far as energy absorption is concerned, is in an unstiffened rectangular diaphragm of small thickness, so that the edge bending strains are minimal. The edge conditions in the unwelded strap-stiffened diaphragms were made essentially the same as those in the unstiffened diaphragms by rounding the inner lower edge

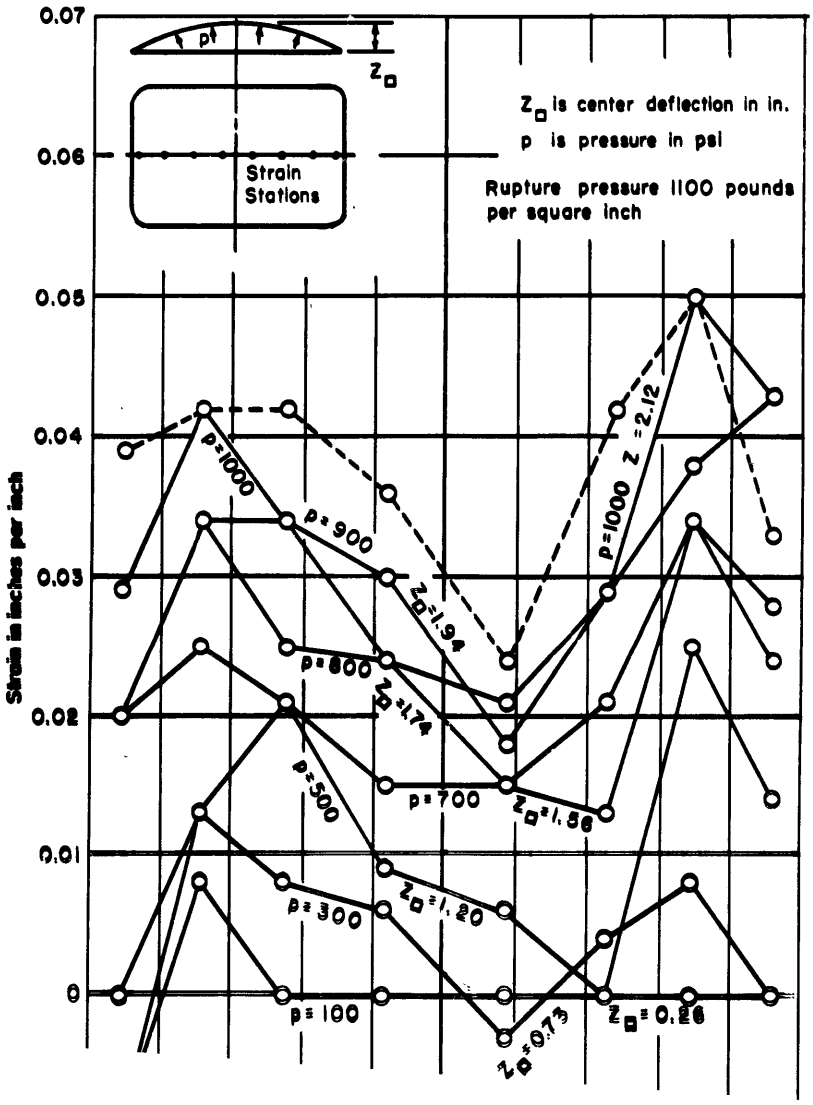

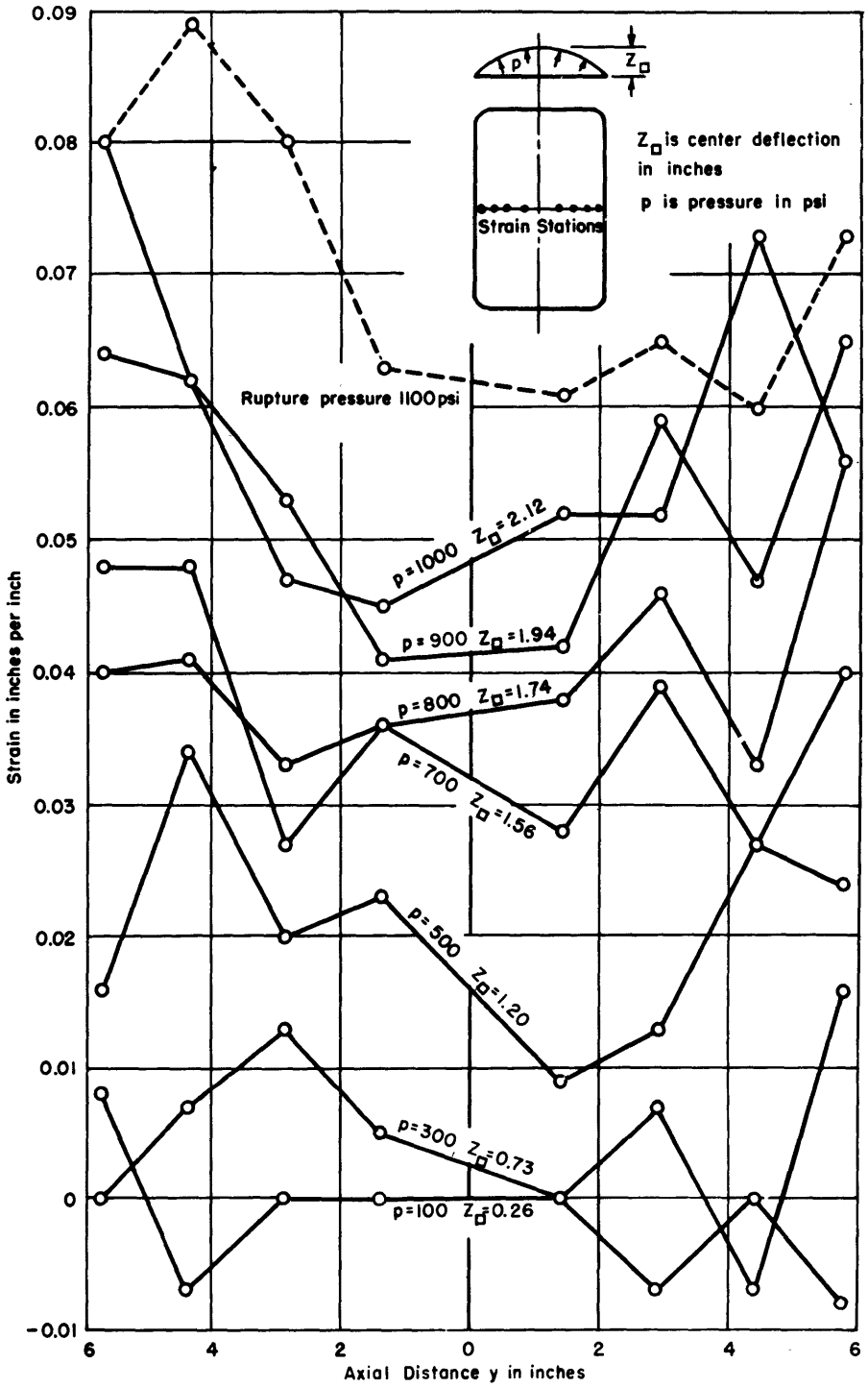

Figure 13b - Strain in Transverse Stiffener

Figure 13 - Strain in Longitudinal and Transverse Unwelded Strap Stiffeners of 1/8-Inch Medium-Steel Diaphragm PS-1, Obverse

The dotted curve is for p = 1100 psi and represents plastic strains only as obtained from elongation measurements made on the diaphragm after it was machined from the compression plate. The other curves represent both plastic and elastic strains for the given pressures as obtained from grid displacement measurements.

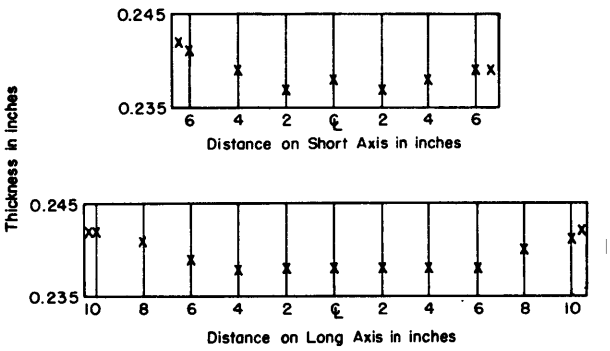

Figure 14a - Final Thickness of Diaphragm P-2, Obverse

The average original thickness was 0.247 inch.

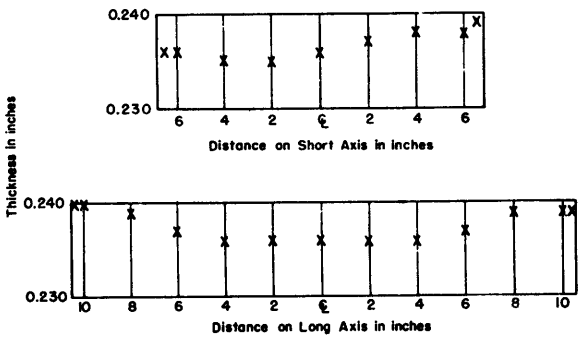

Figure 14b - Final Thickness of Diaphragm P-2, Reverse

The average original thickness was 0.244 inch

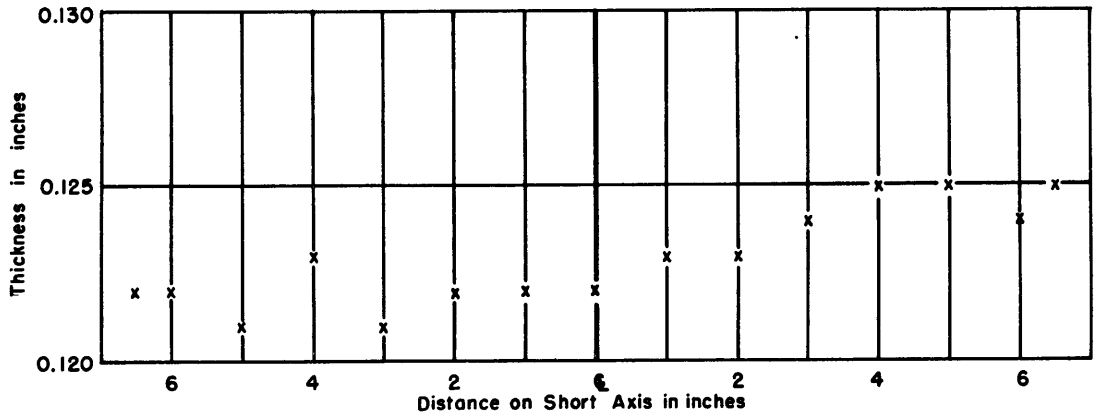

Figure 14c - Final Thickness of Strap of Diaphragm PS-4, Reverse

The average original thickness was 0.133 inch.

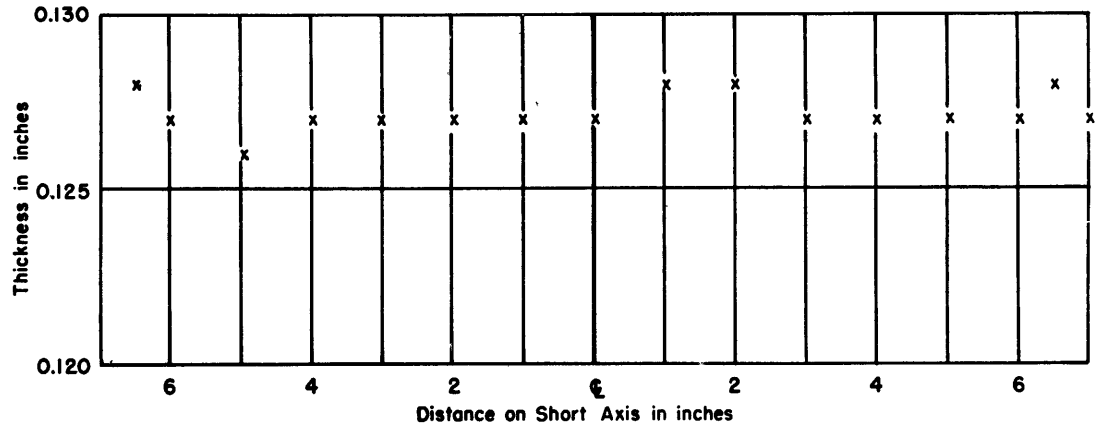

Figure 14d - Final Thickness of Strap of Diaphragm PS-4, Obverse

The average original thickness was 0.130 inch.

Figure 14 - Final Thicknesses

of the strap. The edge problem for the welded strap-stiffened diaphragms was somewhat different. The welded strap stiffeners of Diaphragms PS-2 were similar to the unwelded stiffeners of Diaphragms PS-1. The edges of the straps were welded to the diaphragms; but the welds were terminated at the ends of the straps, thus creating a structural discontinuity in an area where maximum strains occurred in the diaphragm. To eliminate this cause of failure the inner edges of the strap structure, which were overlaid by the clamping frames, were welded to Diaphragms PS-3 (Figure 19). However, by welding the inner edge of the stiffener structure to the diaphragm a double thickness was produced where the diaphragm was

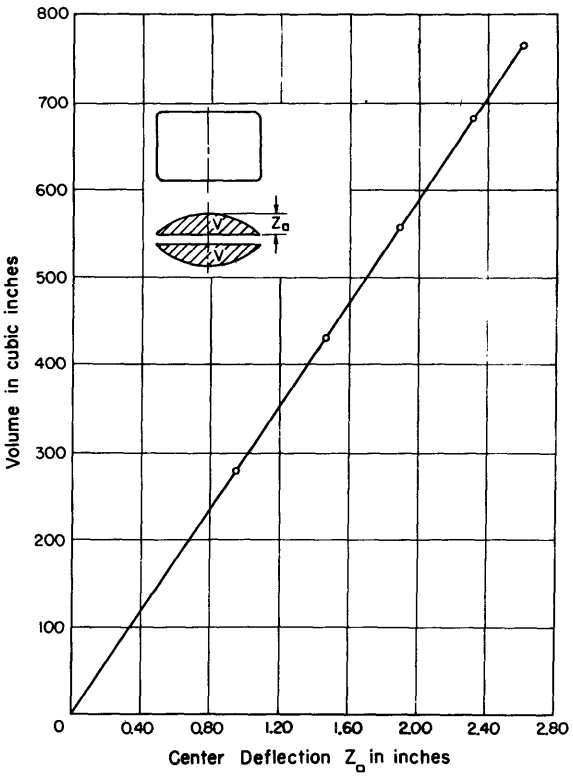

Figure 15a - Volume Change of 1/8-Inch Medium Steel Diaphragms P-3

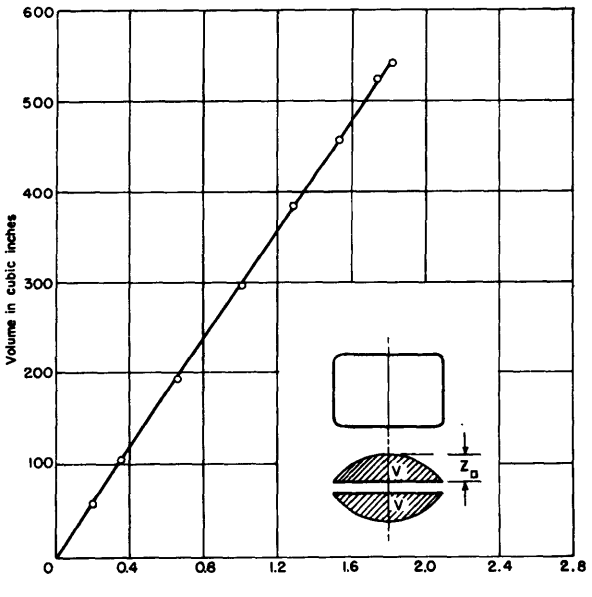

Figure 15b - Volume Change of 1/4-Inch Laminated Medium-Steel Diaphragms P-7

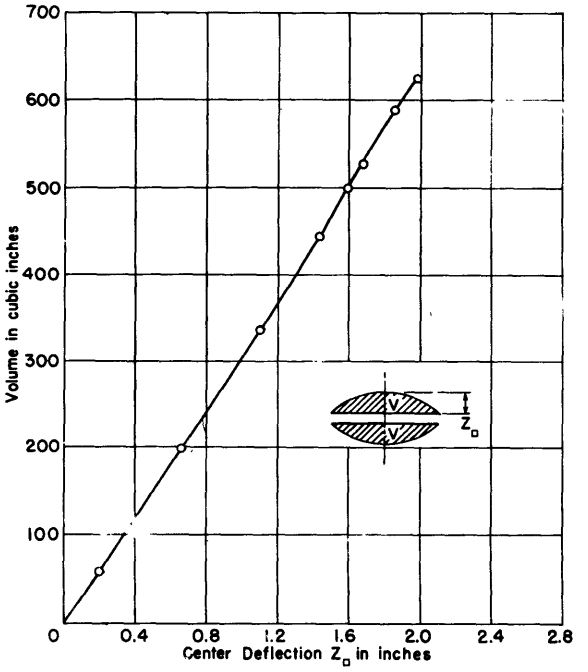

Figure 15c - Volume Change of 1/8-Inch Medium-Steel Diaphragms PS-3 with Welded Strap Stiffeners

Figure 15 - Volume Changes Plotted against Center Deflection

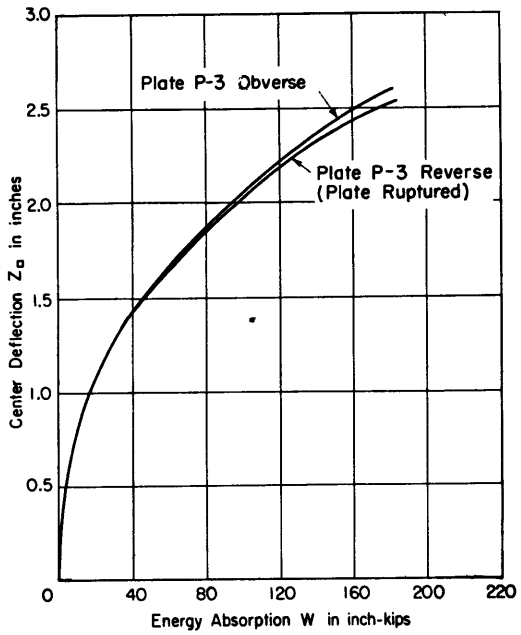

Figure 16a - Energy Absorption of 1/8-Inch Medium-Steel Diaphragms P-3

bent over the rounded edge of the clamping frame. As a result of these design factors Diaphragms PS-1 and PS-2 are directly comparable while the extra rigidity resulting from the double thickness should be considered when Diaphragms PS-3 and PS-5 are compared with other diaphragms.

Diaphragms PS-1, equipped with unwelded strap stiffeners, reached a higher pressure before rupture and absorbed more energy per pound than any of the other stiffened diaphragms. Diaphragms PS-3 with welded strap stiffeners were almost as good as Diaphragms PS-1 as regards rupture pressure and energy

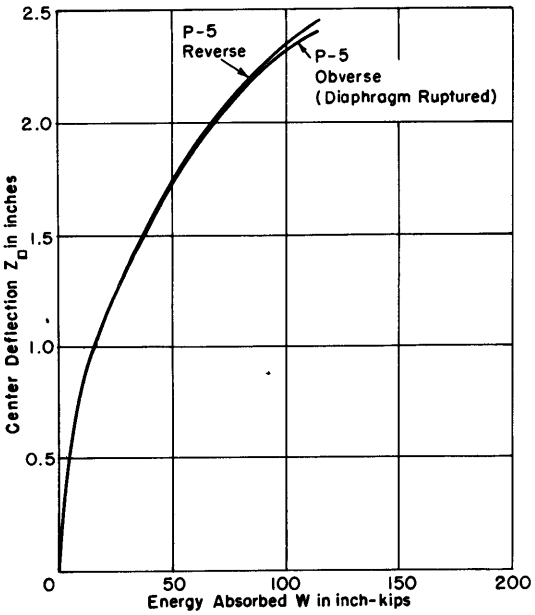

Figure 16b - Energy Absorption of 1/8-Inch Laminated Medium-Steel Diaphragms P-5

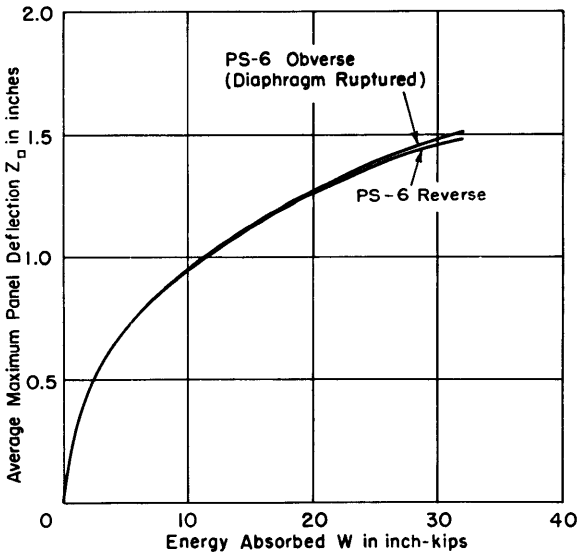

Figure 16c - Energy Absorption of 3/4-Inch Furniture-Steel Diaphragms PS-6 with Transverse Bar Stiffener

Figure 16 - Energy Absorption Plotted against Center Deflection for Various Diaphragms

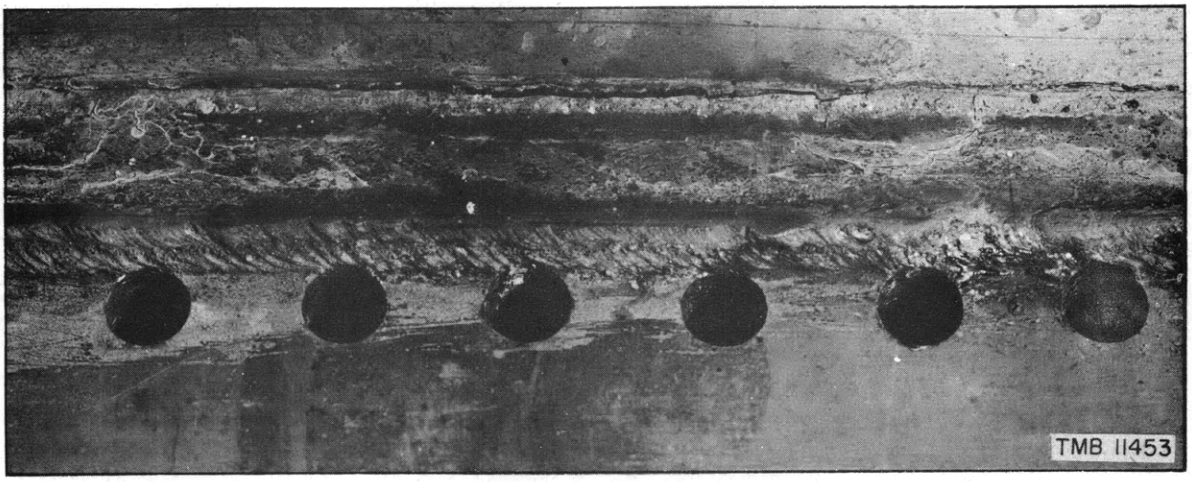

Figure 17 - Diaphragm P-3, Reverse, Showing Rupture at a Pressure of 950 psi

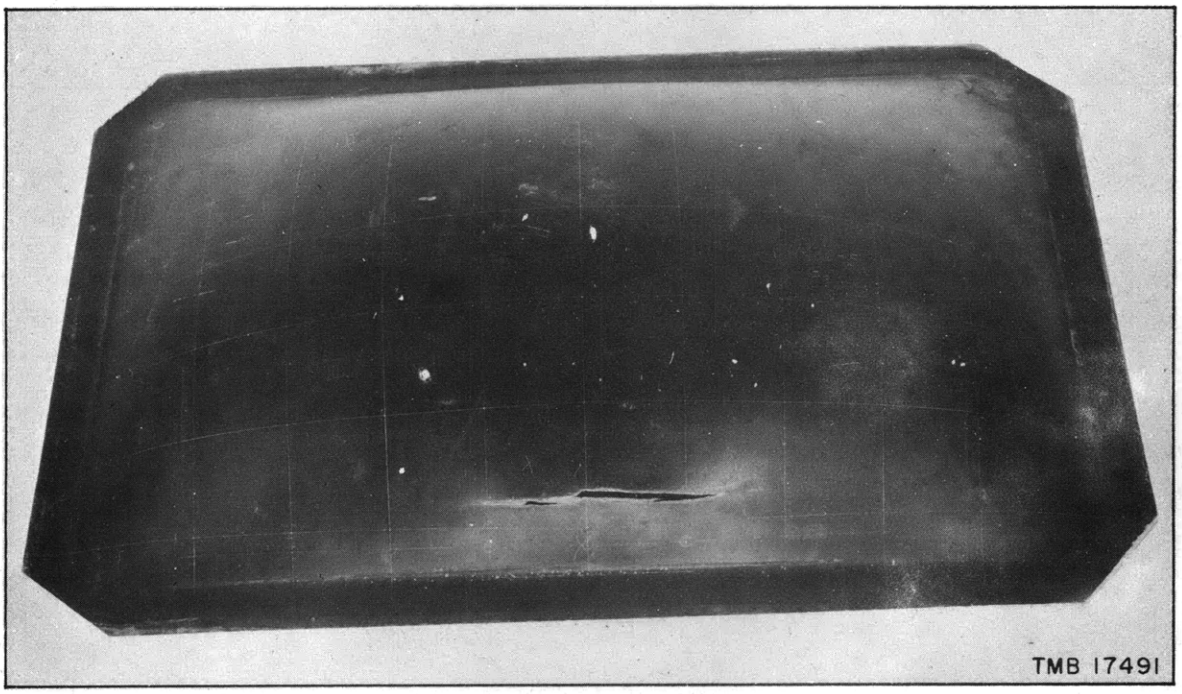

Figure 18 - Diaphragm P-6, Reverse, Showing Rupture at a Pressure of 435 psi

absorption but they had greater rigidity. Failure of Diaphragms PS-5 at the low pressure of 675 psi was caused by a blow hole in the strap weld near the center of the diaphragm. Thus the performance of diaphragms with welded stiffeners depends on the quality of the welding and may vary considerably.

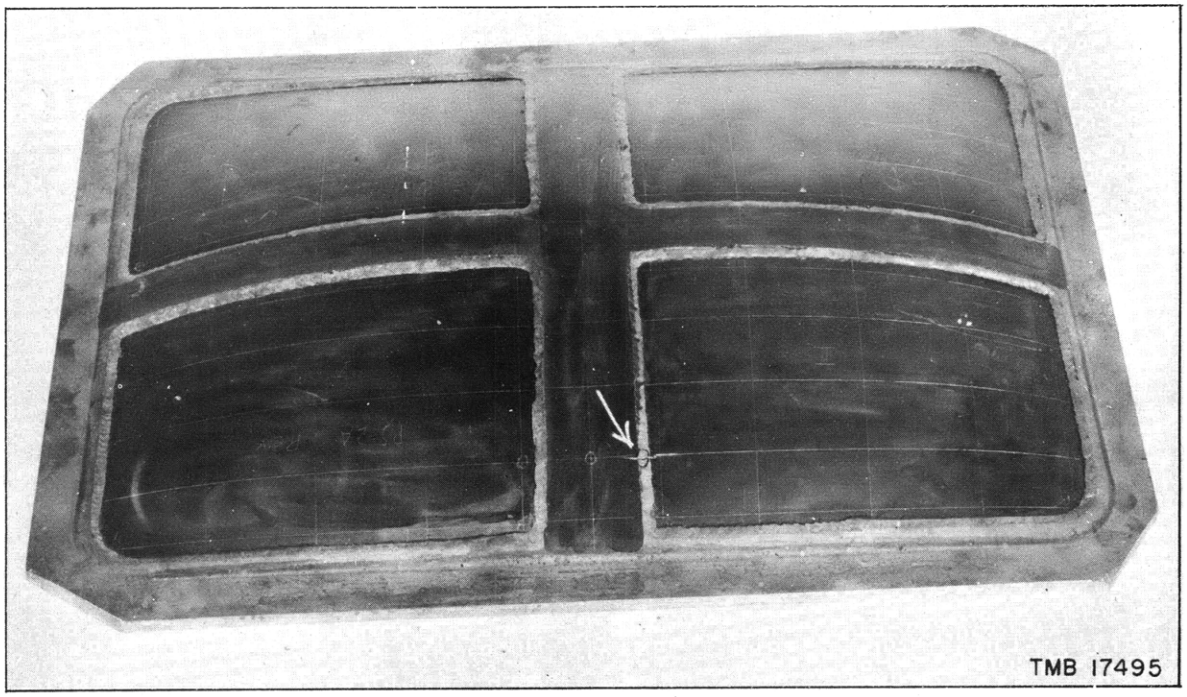

Figure 19 - View of Medium-Steel Diaphragm PS-3,
Reverse, After Testing

The nominal thickness of the diaphragm was 1/8-inch, with edge-welded straps of the same nominal thickness. Rupture occurred at the location shown by the arrow, at a pressure of 1075 psi. The primary rupture was in the fillet weld and then spread into the strap stiffener and plate.

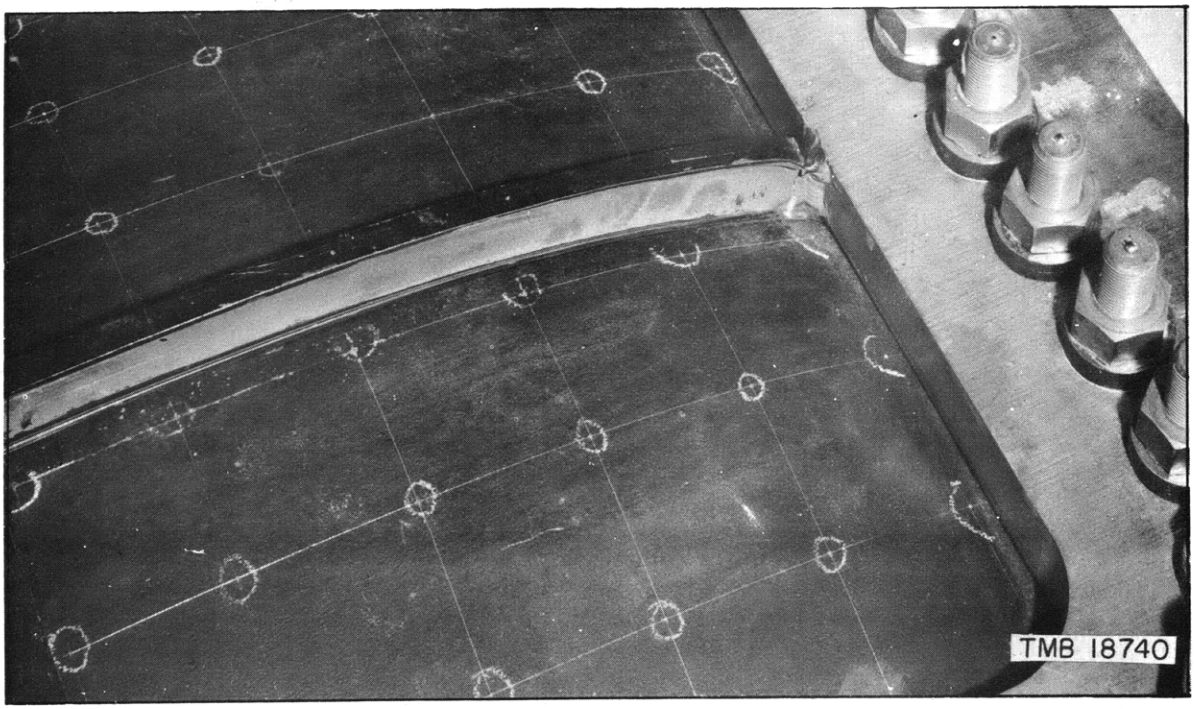

Figure 20 - Enlarged View of Failure of Diaphragms PT-1 in
Web of Stiffener at the Clamping Frame

The tee-stiffened diaphragms, PT-1, PT-2, and PT-3, failed at lower pressures and absorbed less energy per pound of weight than the strap-stiffened diaphragms.

Table 3 sets forth some comparisons of the results of single unstiffened diaphragms and double laminated diaphragms of approximately equivalent thickness. In the case of single Diaphragms P-2 and the double Diaphragms P-7 no significant contrast in performance under test is evident. Diaphragms P-1 are not tabulated because the premature failure at the edge weld was not typical of the group. The unit energy absorbed by the double diaphragm was 4 1/2 percent greater than that absorbed by the single diaphragm, where the ultimate strength of the material in the latter was 6 percent higher. The nominal thickness of these two diaphragms was 1/8 inch.

Single Diaphragms P-3 and P-8 show no significant differences in performance as indicated in Table 3. Using these diaphragms as a basis for comparing the double Diaphragm P-5, it is noted that unit energy absorbed by the double diaphragm was over 40 percent less than that absorbed by the single diaphragms, yet the ultimate strengths of the material of the double diaphragm were only 30 and 16 percent less than those of the single diaphragms P-3 and P-8, respectively.

From all practical considerations a double laminated diaphragm would be expected to have greater center deflection and greater unit energy absorption than a single diaphragm of similar material and equivalent thickness. The two comparisons set forth above offer no indication that the double laminated diaphragm is superior to the single one of equivalent thickness and similar material; instead the limited data indicate performance to the contrary.

COMPARISON OF EXPERIMENTAL RESULTS WITH THEORY

A theory which accounts for the behavior of thin, clamped, circular or rectangular diaphragms under increasing hydrostatic pressure was developed in a previous report.[3] The theory is based on two assumptions, one concerning the shape of thin, clamped, circular or rectangular diaphragms under hydrostatic pressure, and the other concerning the invariance of energy absorption as a function of the areal strain of thin diaphragms. The tension, or force per unit length, in a biaxially stressed diaphragm, is approximately constant because of the balancing of the strain-hardening of the material with the reduction in thickness as the stress increases.

The relation between the center deflections of two diaphragms of like material and the pressures which produce these deflections is expressed by simple algebraic equations involving the physical dimensions of the diaphragms. Thus, if the pressure-deflection function of a diaphragm is known,

the diaphragm may be used as a model or "equivalent" diaphragm by which the theory may be applied for the prediction of pressure and center deflection for any other circular or rectangular diaphragm of the same material. By use of measured values of ultimate stress obtained from a standard tensile test, the equations may be extended to diaphragms of different materials. The energy absorbed in the plastic deflection of any circular or rectangular diaphragm may also be predicted.

In the following sections results predicted by this theory are compared with experimental results obtained in the present tests on rectangular diaphragms. It will be well to remember during these comparisons that the theory of rectangular diaphragms is often comparative rather than absolute, and thus some freedom of choice of the stress value σ is allowable. This choice is exercised mainly in the use of the approximate equation for energy absorbed where approximate values of energy are compared with measured experimental values.

THE VOLUME EQUATION

An equation for the volume displaced by a rectangular diaphragm as it deflects under hydrostatic pressure was developed in Reference 3. This equation (based on the assumption that the diaphragms deflect parabolically) is a convenient expression of volume in terms of original area and center deflection of the diaphragm.

The actual measured final volumes for sixteen diaphragms of the present test are compared with the volumes computed by Gleyzal's[3] volume equation

$$V = \frac{16}{9} a_1 a_2 Z_\square$$

for a rectangular diaphragm, where a_1 and a_2 are the half-length and half-width of the diaphragm and $Z_\square$ is the center deflection. Table 4 shows the final measured and computed volumes and the percentage of variance of the computed volumes from the measured final volumes. The values of volume variance for the first group of diaphragms, P-1 to P-4, had an average deviation of 2.83, while the average deviation of the second group, P-5 to P-8, was 1.11. Better volume-measuring methods were used for the second group of diaphragms, which may account for the more consistent results.

The volume equation was tested over the range of test conditions for each of the diaphragms P-5 to P-8. The volume was computed for each center deflection recorded during the test on these diaphragms. The computed volumes were compared with the actual measured volumes (obtained by metering the pressure fluid) corresponding to each center deflection and the percent variance was computed in each case. Among the four pairs of diaphragms tested, the

volume variances for all conditions observed ranged from 4.6 percent to 23.7 percent. There was no pattern in these variations. The average volume variance for 23 sets of observations was 13.2 percent. The computed volume was always lower than the measured volume for a given center deflection. It may be said that the volume equation is reliable within at most 15 percent.

EQUIVALENT RADIUS: THE FUNCTION ϕ

According to Reference 3 two diaphragms are in corresponding states if their areal strains are equal. One diaphragm may be circular and one may be rectangular. This relation is expressed in the equation

$$\frac{Z_o^2}{a_o^2} = \frac{16}{45} Z_\square^2 \left(\frac{1}{a_1^2} + \frac{1}{a_2^2}\right)$$

where Z_o is the center deflection of the circular diaphragm, in inches,
a_o is the radius of the circular diaphragm, in inches,
$Z_\square$ is the center deflection of the rectangular diaphragm, in inches,
a_1 is the semi-major axis of the rectangular diaphragm, in inches, and
a_2 is the semi-minor axis of the rectangular diaphragm, in inches.

The rectangular and circular subscripts refer to rectangular and circular diaphragms respectively. The above equation suggests a definition for equivalent radius $a_\square$ of a rectangular diaphragm which can be expressed as

$$\frac{1}{a_\square^2} = \frac{16}{45}\left(\frac{1}{a_1^2} + \frac{1}{a_2^2}\right) \quad \text{or} \quad a_\square = \frac{a_1 a_2}{4}\sqrt{\frac{45}{a_1^2 + a_2^2}}$$

The equivalent radius is a term that allows direct comparison of rectangular diaphragms with circular diaphragms. The appropriate relations for center deflection, energy absorption, and pressure may be stated, from Reference 3, to be as follows:

If $\frac{Z}{a} = \frac{Z_\square}{a_\square} = \frac{Z_o}{a_o}$

then

$$\frac{W}{\overline{W}} = \frac{W_\square}{4a_1 a_2 \sigma_\square h_\square} = \frac{W_o}{\pi a_o^2 \sigma_o h_o} = \phi\left(\frac{Z}{a}\right)$$

and

$$\frac{1}{2} P = \frac{4}{9} \frac{p_{\square} a_{\square}}{\sigma_{\square} h_{\square}} = \frac{1}{2} \frac{p_o a_o}{\sigma_o h_o} = \phi'\left(\frac{Z}{a}\right)$$

where W, $W_{\square}$ or W_o is the energy absorbed by a diaphragm under increasing pressure, in inch-pounds,

$\overline{W}$ is equal to $4\sigma_{\square} h a_1 a_2$ or $\sigma_o h \pi a_o^2$,

$a_{\square}$ is the equivalent radius of the rectangular diaphragm, in inches,

$h_{\square}$ or h_o is the original thickness of the diaphragm, in inches,

p is the applied hydrostatic pressure, in pounds per square inch,

$\sigma_{\square}$ or σ_o is a stress representing the strength of the diaphragm material measured in the same way for both diaphragms, e.g., it may be the "ultimate" stress,

P and $\left(\frac{Z}{a}\right)$ are quantities defined by the equations.

The rectangular and circular subscripts refer to rectangular and circular diaphragms respectively, and ϕ is the same function for all thin clamped rectangular or circular diaphragms.

Using the basic relation

$$\frac{W}{\overline{W}} = \phi\left(\frac{Z}{a}\right)$$

the function ϕ may be subjected to experimental evaluation as a check on the theory, since this function should be the same for all thin, clamped, rectangular or circular diaphragms. The establishment of the experimental value of the function ϕ would then make the prediction of energy absorption for any rectangular or circular diaphragm a simple matter of substituting known and assumed values in the above equation.

From the results of tests on a series of diaphragms, data may be assembled by which a curve of the function ϕ may be constructed. For each diaphragm nondimensional values of energy $\left(\frac{W}{\overline{W}}\right)$ and equivalent deflection $\left(\frac{Z}{a}\right)$ may be obtained for each hydrostatic pressure stage of a diaphragm test, and with the values of the latter as abscissa and values of energy as ordinates a curve of the function ϕ is generated; such a curve is shown in Figure 21. This figure was constructed from the results of sixteen rectangular diaphragms tested. The plotted points on the curve represent values of $W/\overline{W}$ and $Z_{\square}/a_{\square}$ computed from the final pressure stage of each of the eight diaphragms P-1 to P-4, and from each pressure stage of each of the eight diaphragms P-5 to P-8.

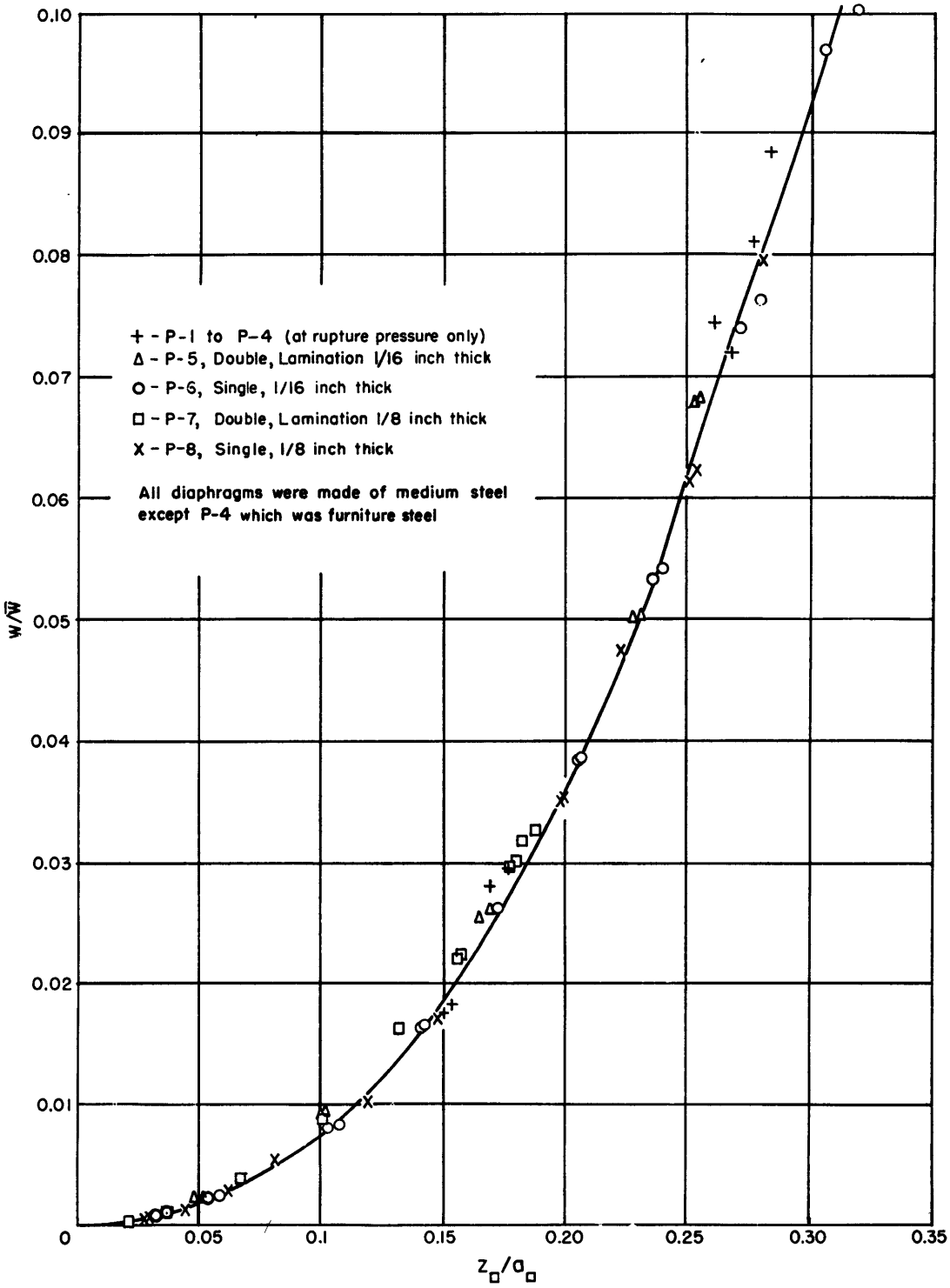

Figure 21 - Curve for the Function ϕ as Expressed by the Relation $\frac{W}{\bar{W}} = \phi \frac{Z_{\square}}{a_{\square}}$

The curve of the function ϕ is useful where it is desirable to predict characteristics of hydrostatic diaphragms without the need of resorting to the delay of actually testing numerous specimens. For a given value of center deflection Z, the factor Z/a may be determined, and the corresponding value of W/$\overline{W}$ may be determined from the curve. The actual energy W which the diaphragm would have absorbed at the assumed center deflection Z may then be determined by calculating $\overline{W}$ from the physical dimensions of the diaphragm and the value of the ultimate strength of the material as determined from a simple coupon tensile test.

EXPERIMENTAL AND THEORETICAL PRESSURE-DEFLECTION CURVES

Figure 22 is a reproduction in part of Figure 3 of Reference 3. It contains two of the four theoretical curves and four of the experimental curves of rectangular diaphragms occurring in Figure 3 of Reference 3 since that reference made advance use of some of the results of the present test. Figure 22 shows experimental results for all but two of the sixteen unstiffened rectangular diaphragms of the present test.

The experimental curves in Figure 22 show that for an "equivalent deflection" Z/a of 0.15 the spread of "equivalent pressures" P for the various diaphragms tested was about 20 percent of the average "equivalent pressure." For an "equivalent deflection" of 0.25 the dispersion was about 25 percent. These dispersion values were somewhat high because of the fact that the values of stress σ_u used in computing the "equivalent pressure" P for Diaphragms P-1 to P-3 were not complete, that is, the values of σ_u used for these six diaphragms were representative of only a pair of diaphragms. The curves in Figure 22 for Diaphragms P-5 to P-8, for which a complete set of values of σ_u was available, were in much closer agreement.

Figure 22 includes also a curve obtained by exact membrane theory for a rectangular diaphragm, whose aspect ratio is 3/2. This curve was obtained by the following procedure. A convenient value for $Z_\square/a_\square$ was assumed, the "equivalent radius" of the rectangular diaphragm $a_\square$ was known, and the corresponding value of the center deflection $Z_\square$ was obtained. The "equivalent pressure" P was determined by use of Equations [19] and [22] of Reference 3. The right-hand member of Equation [22],

$$p_\square = 4.84 \frac{\sigma_\square h_\square Z_\square}{a_\square^2}$$

was substituted for $p_\square$ in Equation [19]

$$P = \frac{8}{9} \frac{p_\square a_\square}{\sigma_\square h_\square}$$

Exploring the data of the remaining diaphragms of this test, P-6, P-7, and P-8, with the approximate equation for energy absorbed, an attempt was made to establish limits of usage for the ultimate and yield strengths when used as values of $\sigma_{\square}$ in the equation for prediction of energies over the test range of the diaphragm. No well-marked limits of usage for these values of $\sigma_{\square}$ were indicated by the energy-variance data, but use of the yield strength for $\sigma_{\square}$ up to 65 percent of the maximum center deflection and the ultimate strength for the remaining 35 percent gave better results than any other percentage combination. This rule gave energy variances from about +25 percent at low diaphragm deflections to plus or minus a few percent at high deflections. The approximate equation for energy absorbed is not reliable when either ultimate or yield strengths are used for $\sigma_{\square}$ at deflections lower than 10 to 15 percent of maximum expected deflection.

CONCLUSIONS

1. The experimental techniques and procedures developed in these tests are considered suitable for testing large rectangular diaphragms 7 feet by 4 1/2 feet.

2. Single unstiffened medium-steel diaphragms with a ratio of equivalent radius to initial thickness ($a_{\square}/h_{\square}$) greater than 80 absorbed more energy per pound of weight than any other diaphragms tested.

3. Double laminated medium-steel diaphragms showed no superiority over single medium-steel diaphragms of equivalent thickness in energy-absorbing qualities.

4. The unwelded strap-stiffened diaphragm failed at a higher hydrostatic pressure and absorbed more energy than any other stiffened diaphragm.

5. The equation for computing the volume displacement of a diaphragm corresponding to a given center deflection may be relied on for accuracy of about 0 and -15 percent.

6. The experimental and theoretical pressure-deflection curves were in good agreement.

7. The approximate equation for energy absorbed gave rather varying results. Results were improved somewhat when the tensile yield strength was used for the value of σ where diaphragm center deflections were under 65 percent of expected maximum. For higher center deflections the tensile ultimate strength was used for the value of σ. With these modifications the equation may generally be said to be reliable to within ± 15 percent. However, its reliability is doubtful for low center deflections based on present applications.

REFERENCES

1. TMB CONFIDENTIAL letter C-S81-3 of 9 September 1943 to BuShips.

2. BuShips CONFIDENTIAL letter C-S81-3(374a) of 16 September 1943 to TMB.

3. Gleyzal, A.N., Ph.D., "Plastic Deformation and Energy Absorption of a Thin Rectangular Plate under Hydrostatic Pressure," TMB Report R-280, January 1945.

4. Mintz, F., "A Summary of Static Deflection Data on Three Series of Plastic Diaphragms," TMB RESTRICTED Report 506, October 1943.

5. Gleyzal, A.N., Ph.D., "Plastic Strain and Deflection Tests on Clamped Circular Steel Plates 20 Inches in Diameter," TMB Report R-142, May 1944.

NAVY-DPPO PRNC WASH D C